공학석사 학위논문

Pyrochemical Electrorefining Studies with Zr and Nb for CANDU Pressure Tube Decontamination into Low Level Wastes

CANDU 압력관 폐기물의 저준위화를 위한 파이로 전해정련 공정연구

2019년 2월

서울대학교 대학원

에너지시스템공학부

정 성 진

Abstract

Pyrochemical Electrorefining Studies with Zr and Nb for CANDU Pressure Tube Decontamination into Low Level Wastes

Seongjin Jeong

School of Energy Systems Engineering
The Graduate School
Seoul National University

Zirconium is a material having low thermal neutron absorption cross section, and high corrosion resistance. Various zirconium alloys obtained by adding niobium in zirconium add to the resistance to hydrogen embrittlement, to overcome a weak point of zirconium metal. It is used in various fields such as pressure tube for CANDU where it operated at very high temperature and high pressure. In spite of these advantages of niobium, Natural Nb-93 results in the mass production of

Nb-94 under high neutron radiation. Nb-94 has a long half-life and beta radioactivity, so it is very costly to dispose of decommissioned pressure tube. With the replacement of pressure tube in the past, 23 tons of pressure tubes have already been discharged of interim storage. As a result of the permanent shutdown of Wolsong nuclear power plant to be made in the future, decommissioned pressure tubes from 115 tons upto 180 tons will be discharged of waste by 2029.

At present, it is not possible to dispose of the pressure tubes as the domestic repository in Gyeong-ju. It is anticipated that if it can be made into LLW through the decontamination process for the pressure tubes, it will be a solution for zirconium alloy decommission waste used in various places including pressure tube and fuel cladding.

For this reason, previous studies have been conducted to decontaminate the zirconium alloys. The surface decontamination research published in 2009 seems to be difficult to separate niobium which is uniformly distributed in the zirconium alloy due to the limitation of the penetration thickness of the decontamination material. Decontamination process with iodine gas is also not preferred due to its high process cost.

The most suitable process is thought to be an electrorefining process. Electrorefining processes such as fluoride and chloride are now being studied. In the case of fluoride, it has advantages to recover the bulk metal particle form of the complex in the electrorefiing process. But, engineering issues like high corrosion and high temperature process are raised. Chloride processes are suitable for commercial processes because they can perform processes with less corrosion problems and lower temperature than fluorides. In the case of chloride salts, zirconium and niobium have disproportionate reactions. So, it should

be studied.

In this thesis, it is explained that the zirconium and niobium are seperated through electrorefining based on the redox behavior of Zr and Nb in chloride salt. For this purpose, the radioactivity of the pressure tube was calculated using ORIGEN-2, the radiation concentration of Nb-94 was determined, and the decontamination factor goal was set to 75,100.

For the electrorefining process, the redox behavior of Zr and Nb in chloride salts were collected by the cyclic voltammetry method. The collected data were confirmed to be consistent with the literature data. Because the oxidation potential of zirconium metal is negative than that of niobium. The oxidation of niobium should be suppressed during process. Based on this, the behavior of each element was first predicted using REFIN, a 1-D electrorefining calculation code, and an electrorefining process using LiCl-KCl-$ZrCl_4$ salt was designed.

In earlier studies, the precipitation behavior of niobium particles was not considered during electrorefining experiments. In this thesis, a basket was added to physically separate niobium particles from zirconium deposits. The deposited materials was uniformly in the basket after experiments, unlike the uneven distribution of the complexes in the salt at in earlier studies. In addition, through the composition analysis using ICP-MS, high purity zirconium was recovered. A decontamination process of CANDU pressure tube disposal wastes through electrorefining was achieved with high decontamination factor of 10,000 to 200,000. The value is sufficiently high for Nb. The results of the experiments were confirmed on a lab scale the model prediction.

In practice, however, a rotating electrode is used to control the

limiting current and diffusion layer. In this case, a flow may occur in the electrolyte and the Nb particle may become contaminated with the Zr deposits. In order to prevent this, an additional basket installation is essential. However, if a basket is installed, the power efficiency becomes lower due to additional potential drop. To solve this problem, CFX-ANSYS was used to simulate the behavior of the particle in the fluid and simulate the potential drop, assuming a cell with some holes in the basket. It was possible to design an efficient electrolytic cell that can overcome the issues through this work.

These findings suggest that pilot-scale and commercial-scale design would result in reduction of more than 28billion KRW and additional costs in long term interim storage facilities will be reduced.

Keywords

Pressure Tube

Zirconium

Niobium

Electrorefining

Student Number

2017-24335

Contents

Chapter 1 Introduction.....1

1.1 Background..... 1

1.2 Problem Statement 5

Chapter 2 Literature Review.....12

2.1 Surface decontamination 12

2.2 Volume decontamination 13

Chapter 3 Research goal and approach 24

3.1 Rationale and Research Goal..... 24

3.2 Research approach 25

Chapter 4 Cyclic Voltammetry Experiments.....19

4.1 Materials and Apparatus..... 27

4.2 Cyclic voltammetry of Zr and Nb in LiCl-KCl 32

4.3 Cyclic voltammetry of Zr and Nb in LiCl-KCl-ZrCl4-NbCl5 36

4.4 Reduction of Thermodynamic data..... 39

Chapter 5 Electrorefining studies 43

5.1 1-D simulation 43

5.2 Electrorefining experiments 53

5.3 Electrorefining Element Flow chart..... 61

Chapter 6 Cell design 63
6.1 Cell Design and Challenging Issue 63
6.2 New design cell 68
6.3 Pilot Cell Design 72

Chapter 7 Conclusions and Future work 76
7.1 Conclusion 76
7.2 Future Work 77

APPENDIX I. ORIGEN-2 INPUT(CANDU Pressure Tube simulation) 79

APPEBDIX II. REFIN INPUT(Chap. 5.1 input) 82

Bibliography 85

Abstract 89

List of Tables

Table 1.1 Zircaloy including Nb components of nuclear power plants 2
Table 1.2 Zr-2.5Nb composition data from ASTM. 3
Table 1.3 Measured and estimated radioactivity of decommissioned P-T KAERI(2011). 6
Table 1.4 Estimated radioactivity of decommissioned P-T KINGS(2015)...6
Table 1.5 Specification of 1st Gyeong-ju repository.....8
Table 1.6 Radioactivity of decommissioned pressure tube after 10yr cooling 11
Table 2.1 Compostiion of deposited Zr on cathode with LiF-KF-ZrF4(T. K. Park et al.).....16
Table 2.2 Composition of deposited Zr on cathode owith LiCl-KCl-ZrCl4(J.Y. Park et al.).....19
Table 2.3 Table 2.3 Composition of deposited Zr on cathode owith LiCl-KCl-ZrCl4(P. H. Kim et al.).....20
Table 2.4 Comparison of each decontamination process for zircaloy 22
Table 4.1 Material purity and manufacturer for experiments.....29
Table 4.2 Geometry and material for cyclic voltammetry 29
Table 4.3 CV experiments table 31
Table 4.4 Diffusion coefficient of Zr in LiCl-KCl 41
Table 4.5 Diffusion coefficient of Nb in LiCl-KCl 41
Table 4.6 Appaerent equilibrium potential of Zr in LiCl-KCl 41
Table 4.7 Appaerent equilibrium potential of Nb in LiCl-KCl 42
Table 5.1 material appaaratus for benchmark problem 44
Table 5.2 1-D simulation material apparatus 50
Table 5.3 Anode composition for 1-D simulation 50
Table 5.4 1-D simulation results at Zr 99.99% recovery rate. 52
Table 5.5 Experiments setups for lab-scale electorefiing 55
Table 6.1 Particle tracking results with flow velocity 65

Table 6.2 Ohmic drop comparison within this simulation 67
Table 6.3 Ohmic drop comparison within this simulation 69
Table 6.4 Wolsong site expiration schedule and mass of pressure tube wastes 72
Table 6.5 Radioactive waste disposal strategy of France 74
Table 6.6 comparison for disposal cost each scenario 75

List of Figure

Figure 1.1 Decay chian of zirconium and niobium 4
Figure 1.2 Schematic diagram of Gyeong-ju LILW repository. 7
Figure 1.3 Radioactiviy of decommissioned pressure tube during cooling time(100yr).. 10
Figure 2.1 Schematic diagram of K. T. Park's experiments setup (2017) 15
Figure 2.2 Deposited Zr on cathode with LiF-KF-ZrF4(T. K. Park et al.) . 16
Figure 2.3 The results of electrorefining two step in LiCl-KCl-LiF 16
Figure 2.4 Deposited Zr on salt and cathode (J.Y. Park et al.)..... 19
Figure 2.5 Deposited Zr on salt and cathode (P. H. Kim et al.) 20
Figure 3.1 Figure 3.1 Schematic diagram for this thesis flow chart 26
Figure 4.1 Glove box used for experiments..... 28
Figure 4.2 Heat geneartor used for experiments..... 28
Figure 4.3 Schemateic cell design for cyclic voltammetry experiments..... 30
Figure 4.4 Cyclic voltammetry scan rate from 0 to – 1.7V (vs. 1 wt. % Ag/AgCl) 500°C LiCl-KCl-ZrCl4(0.8 wt. %)..... 33
Figure 4.5 Linearity confirmation peak current vs scan rate 33
Figure 4.6 Cyclic voltammetry result of Zr in LiCl-KCl-NbCl5 (0.32wt.% of NbCl5) with scan range from -1.3V to 1.0V (vs. 1 wt% Ag/AgCl) with W electrodes at 500°C..... 35
Figure 4.7 Linearity confirmation peak current vs scan rate 35
Figure 4.8 Cyclic voltammetry result of Zr and Nb in LiCl-KCl-ZrCl4 (1 wt%)-NbCl5(0.1 wt%) with scan range from -1.3V to 1.0V (vs. 1 wt% Ag/AgCl) with W electrodes at 500°C 37
Figure 4.9 Linearity confirmation peak current vs scan rate 37
Figure 4.10 Oxidation peak difference for each elements(Zr and Nb) by cyclic voltammetry..... 38
Figure 5.1 schematic diagram of experiments benchmark problem 44
Figure 5.2 UCl3 compostion in salt comparison for benchmark and experiment..... 45

Figure 5.3 MgCl2 compostion in salt comparison for benchmark and experiment 45
Figure 5.4 GdCl3 compostion in salt comparison for benchmark and experiment 46
Figure 5.5 Each element compostion in salt comparison for benchmark and experiment 46
Figure 5.6 Figure 5.6 Cell design for 1-D simulation 49
Figure 5.7 DF vs Zr recovery rate 52
Figure 5.8 materials used for electrorefining experiments cell design 53
Figure 5.9 deposited Zr and salt after electrorefining in previous study 57
Figure 5.10 deposited Zr and salt after electrorefining in this study 57
Figure 5.11 deposited Zr composition measred by ICP-MS and XRD measured data in experiment #1 58
Figure 5.12 deposited Zr composition measred by ICP-MS and XRD measured data in experiment #2 59
Figure 5.13 deposited Zr composition measred by ICP-MS and XRD measured data in experiment #3 59
Figure 5.14 For each condition related to Nb particle effect control 60
Figure 5.15 Element flow chart for electrorefining 62
Figure 6.1 Flow velocity distribution around rotating electrodes 64
Figure 6.2 Nb particle tracking with flow velocity by rotating electrode 65
Figure 6.3 ohimc drop path 66
Figure 6.4 Potential distribution on cathode 67
Figure 6.5 Basekets around electrodes with holes 68
Figure 6.6 Potential distribution on cathode 69
Figure 6.7 Flow velocity comparision around anode 70

Chapter 1. Introduction

1.1 Background

In Korea, Wolsong unit #1 and Kori unit#1 have been shut-down for retirement. Wolsong unit#1 contains CANDU pressure tubes that correspond to the reactor vessel playing the most important role for operation and safety assurance. The CANDU pressure tube is made of Zr-2.5Nb alloy which can endure corrosion and hydrogen damages under very high pressure, high temperature and high radiation. But, at very high neutron fluence, some of natural niobium (100% Nb-93) and zirconium are transmuted to radioactive isotope Nb-94 which emits beta radiation with very long half-life (20,300 year). Also, a calandria tube surrounding each pressure tube made of Zircaloy-2 makes Nb-94 from the transmutation of Zr-91 and Zr-92.

Total waste mass of pressure tube and calandria tube per one CANDU-6 nuclear power plant (NPP), is about 23 tons and 8 tons, respectively. Since there are 4 unit of CANDU-6 NPPs at Wolsong site, 150~180 tons of wastes will be produced. Wolsong unit #1 already discharged Zircaloy wastes from tube replacement after 30 years of operation. The Nb-94 activity of pressure tubes and calandria tubes from Wolsong exceeds the regulatory limit of existing waste repository by several orders of magnitude. Hence they are identified as intermediate level waste that cannot be disposed of at Gyeong-ju LILW repository.

Table 1.1 Zircaloy including Nb components of nuclear power plants

Alloy	Nb wt%	Component	Reactor Type
ZILRO	1	Cladding	PWR
Zr-2.5Nb	2.4-2.8	Pressure Tube	CANDU
E110	0.9-1.1	Cladding	VVER
E125	2.5	Pressure Tube	RBMK
E635	0.8-1	Structural component	VVER
M5	0.8-1.2	Structural component	PWR

Alloy	Nb wt%	Component	Reactor Type
HANA 3	1.5	Cladding	PWR
HANA 4	1.5		
HANA 5	0.4		
HANA 6	1.1		

Table 1.2 Zr-2.5Nb composition data from ASTM

Element	Concentration(%)
Zirconium	97.5
Niobium	2.5
Iron	0.15

Impuritiy	Concentration(%)
Aluminum	0.0075
Boron	0.00005
Cadmium	0.00005
Carbon	0.027
Chromium	0.01
Cobalt	0.002
Copper	0.005
Hafnium	0.005
Hydrogen	0.001
Magnesium	0.002
Manganese	0.005
Molybdenum	0.005
Nickel	0.007
Nitrogen	0.0065
Phosphorus	0.002
Silicon	0.01
Tin	0.005
Tungsten	0.005
Titanium	0.005
Uranium	0.00035

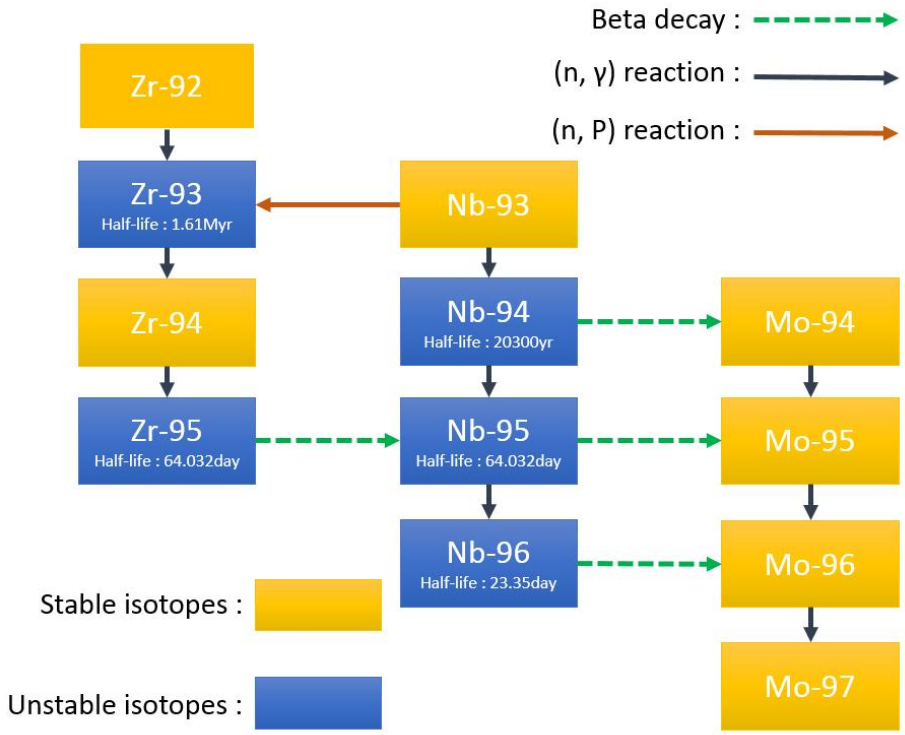

Fig. 1.1 Decay chian of zirconium and niobium

According to tentative national waste disposal plan, the ILW can be disposed of at future High Level Waste (HLW) site that is not yet established. It is undesirable and costly to store large amount of Zr over long period of time. For this reason, it is proposed that Zr alloys wastes are better be decontaminated into LLW for their disposal at Gyeong-ju repository. But, the radioactivity of pressure tube (Zr-2.5Nb) is very high compared with low level waste limit. For this reason, high performance electrorefining process must be developed by both experiments and modeling to separate niobium from zirconium.

1.2 Problem Statement

1.2.1 Irradiated Pressure Tube and Repository

The radioactivity of irradiated CANDU pressure tube from Wolsong #1 was measured and estimated by Korean Atomic Energy Research Institute(KAERI). This result shows that measured radioactivity of irradiated CANDU pressure tube is from 4.334E+06 Bq/g to 8.708E+06 Bq/g, whereas estimated radioactivity of irradiated CANDU pressure tube is from 3.16E+06 Bq/g to 9.95E+06 Bq/g. A good agreement is found.

According to Korea's waste classification standard, the upper limit for low-level waste is 1.11E + 02 Bq/g for Nb-94. It has been confirmed that the radioactivity of decommissioned pressure tube exceeds criteria of intermediate wastes 10,000 times or more. Also, it was confirmed that the estimated radioactivity of decommissioned pressure tube using the results of MCNP and ORIGEN made in KINGS(2015) exceeded the criteria of disposal of pressure tube by more than 10,000 times.

Table 1.3 Measured and estimated radioactivity of decommissioned P-T KAERI(2011)

Location	Measured (Bq/g)	Estimated (Bq/g)
EP4	4.334E+06	3.16E+06
EP34	6.519E+06	6.34E+06
EP3	8.708E+06	9.95E+06

Table 1.4 Estimated radioactivity of decommissioned P-T KINGS(2015)

Nuclide	Specific Activity(Bq/g)	
	Pressure Tube	Calandria Tube
Co-60	1.1.4E+06	8.38E+05
Ni-59	2.52E+02	8.41E+03
Ni-63	3.59E+04	1.21E+06
Nb-94	1.25E+06	1.94E+02

Fig 1.2 Schematic diagram of Gyeongju LILW repository

The 1st Gyeong-ju LILW Disposal Repository, which was completed in 2014, is the only place where the final disposal of LILW is currently possible in the Republic of Korea. However, Nb-94 radioactivity of decommissioned pressure tube wastes is very high, it is virtually impossible to dispose of it. The disposal limit of radioactivity is 1.11E+02Bq/g, which is equivalent to the criteria of LLW standard. Even if the disposal radioactivity limit is not considered, the total amount of radioactive of the disposal site is 9.72E + 10 Bq / g. Therefore, when considering the radioactivity of the pressure tube conducted in the precedent study, only 10kg pressure tube can be disposed of. As the total mass of CANDU pressure tube waste in the Republic of Korea is expected to be between 120 and 180 tons, there is a possibility that only about 1% of pressure pipes will be disposed of Gyeongju repository.

Table 1.5 Specification of 1st Gyeong-ju repository

Index	Value
Area	2,140,000 ㎡
Inventory	100,000 drums
Disposal method	Cave
Radioactivity limit	1.11E+02 Bq/g
Inventory limit	9.72E+10 Bq

1.2.2 ORIGEN-2 Calculation

Based on the above results, the radioactivity of the pressure tube using ORIGEN-2 was calculated to set the target value for the decontamination study of the pressure tube. The assumptions used to calculate this were the expiration time of the pressure tube design life of 30yr, the neutron flux of 1E + 14, the library used CANDUSEU, and the composition of the pressure tube ASTM data base. The result is shown in Figure 1.3. According to the results, the radioactive concentration of C-14, Co-60 and Nb-94 exceeds the disposal limit. However, since the half-life of Co-60 is short, the radioactivity decreases below the disposal criteria after 10-yr cooling. In the case of C-14, carbon is not recovered because of its low reactivity during process using electrorefining.

Nb-94 shows a radioactivity of 8.34E + 06 Bq / g based on 10yr cooling. Based on this, it is confirmed that the fact of decontamination

required for the pressure tube is about 75,100, and the target of obtaining the decontamination factor for taking it account engineering margin is set at 100,000.

$$\text{Decontamination Factor(DF)} = \frac{\text{Con. of initial isopotes}}{\text{Con. of decontamination isopotes}}$$

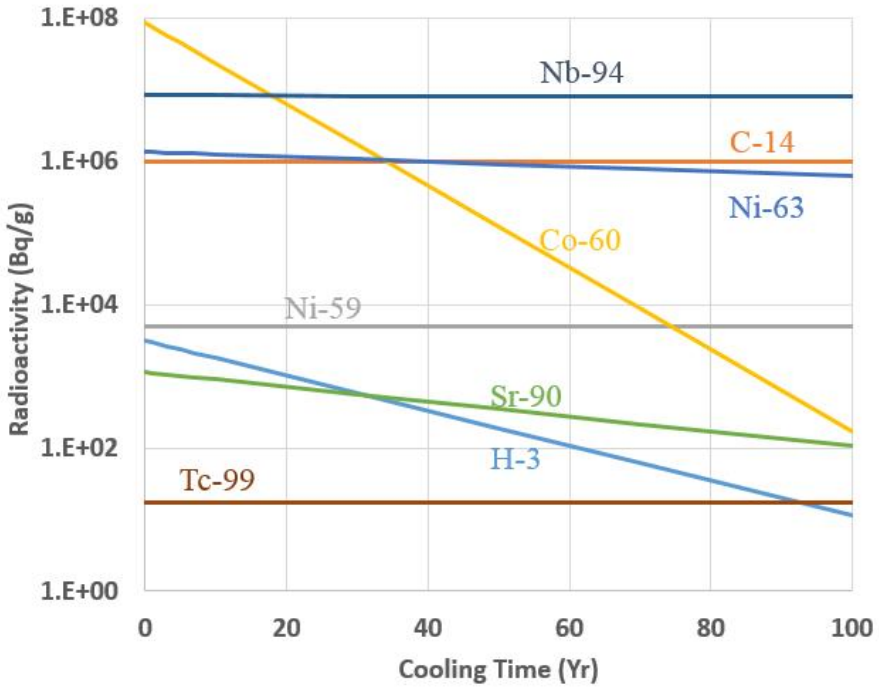

Figure 1.3 Radioactiviy of decommissioned pressure tube during cooling time(100yr)

Table 1.6 Radioactivity of decommissioned pressure tube after 10yr cooling

Isotoptes	**Radioactivity of P-T (10yr Cooled) (Bq/g)**	**Gyeong-ju repository disposal criteria (Bq/g)**	**DF**
H-3	1.79E+03	1.11E+06	1.61E-03
C-14	9.86E+05	2.22E+05	4.44E+00
Co-60	2.36E+07	3.70E+07	6.38E-01
Ni-59	4.91E+03	7.40E+04	6.64E-02
Ni-63	1.26E+06	1.11E+07	1.14E-01
Sr-90	9.09E+02	7.40E+04	1.23E-02
Nb-94	8.34E+06	1.11E+02	7.51E+04
Tc-99	1.75E+01	1.11E+03	1.58E-02

Chapter 2 Literature Review

In that chapter, earlier studies on the decontamination process for the disposal of pressure tube waste have been reviewed. Surface decontamination and volume decontamination were studied. The most appropriate previous study was selected for the disposal of the pressure tube from the literature review.

2.1 Surface decontamination

T. S. Rudisill studied to decontaminate irradiated Zircaloy cladding by using concentrated hydrofluoric acid (HF) to remove cladding surface (Rudisill, 2009). In this study, high decontamination effect of Co-60, Sr-90 and Cs-137 was demonstrated by surface decontamination, indicating that decontamination can be performed at a lower level than the US class C LLW classification standard. However, in this study, fission products deeper than 100 micrometers do not exhibit high decontamination effects despite decontamination. The zirconium-niobium alloy is composed of internally uniform niobium elements. Therefore, it is not suitable for the decontamination of zirconium-niobium alloy requiring high decontamination factor.

2.2 Volume decontamination

The volume decontamination process for zirconium is largely divided into an Iodination process and a molten salt electrorefining process.

2.2.1 Iodination process

The Iodination process consists of two stage processes using iodine gas. In the first stage, Zr is reacted with iodine gas to produce ZrI_4, a volatile substance.

$$\mathbf{Zr + 2I_2 \rightarrow ZrI_4 \text{ at } 300\sim500^\circ C}$$

In this process, elements such as Nb and Fe can react with iodine, but when the temperature exceeds 300 ° C, they are decomposed into a metal state. The ZrI_4 thus produced is collected and enters the second stage. In this reaction, ZrI_4 is separated into Zr and I_2 at temperatures above 1,100 ° C.

$$\mathbf{ZrI_4 \rightarrow Zr + 2I_2 \text{ at } >1{,}000^\circ C}$$

E. D. Collins conducted several zirconium recovery experiments using non-radioactive zircaloy samples and confirmed that Zr can be recovered with high purity. However, the iodination process has some difficult problems. Since ZrI_4 has high reactivity with H_2O, it is necessary to construct a chamber that has very strong resistance to

moisture when it enters a large-scale process. In addition, since a long reaction time is required in the step of separating ZrI_4 into Zr, the efficiency of the decontamination process on the commercial scale is impaired.

2.2.2 Electrorefining in fluoride(-chloride) salts

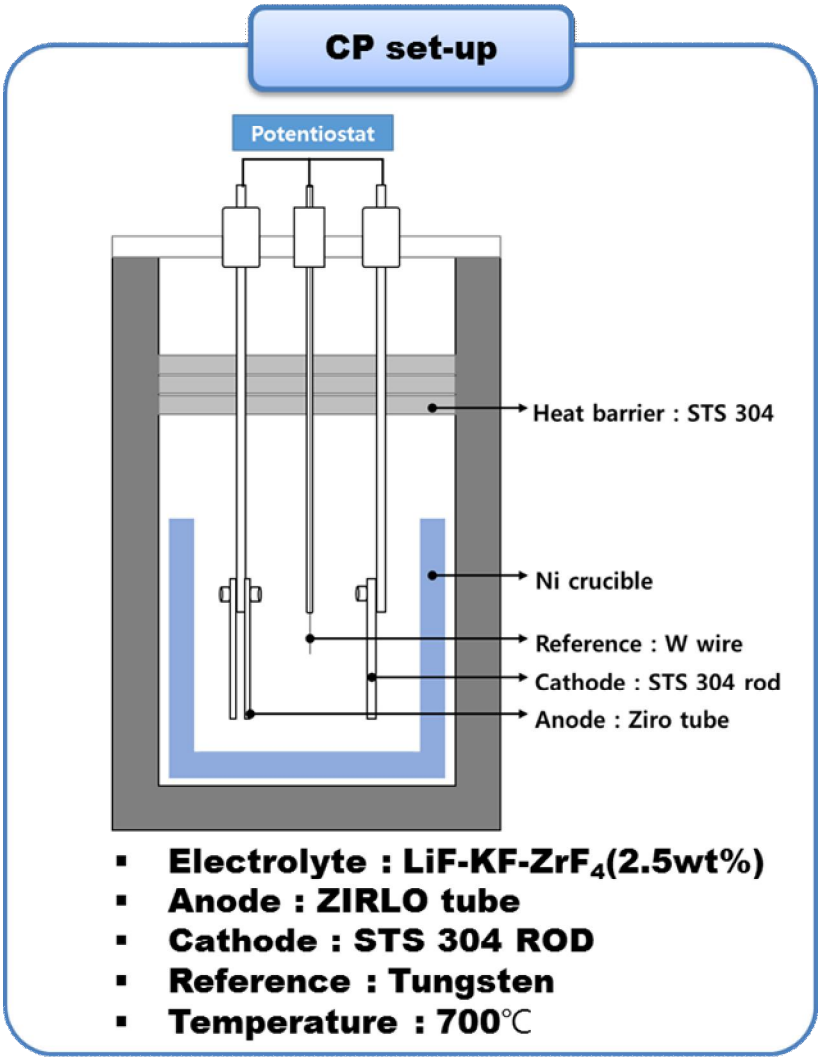

Figrue 2.1 Schematic diagram of experiments setup (T. K. Park et al.)

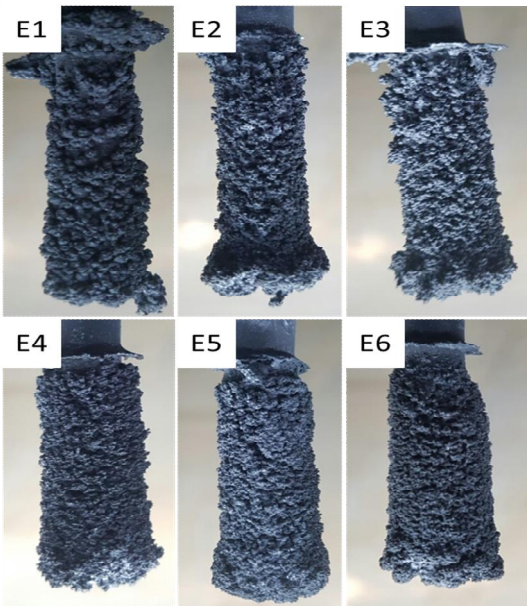

Figrue 2.2 Deposited Zr on cathode with LiF-KF-ZrF_4(T. K. Park et al.)

Table 2.1 Compostiion of deposited Zr on cathode with LiF-KF-ZrF4(T. K. Park et al.)

Element	Concentration(ppm)
Zirconium	999,966.74(99.99%)
Tin	20.46
Tungsten	10.33
Platinum	9.80
Chromium	7.55
Nickel	5.51

The Zr (IV) -> Zr (O) one-Step reduction reaction occurs in salts containing fluoride. Therefore, fluoride salt has less disproportionate reaction than Chloride salt. At Chung-nam University, zirconium electrorefining experiment using fluoride salt was performed. LiF-KF-

ZrF4 salt was used for electrorefining, as the zirconium alloy ZIRLO tube was used, and the experiment temperature was 700 ° C.

As a result, 99.99% or more of pure zirconium was obtained, and the DF of Nb was found to be more than 333.

Zirconium alloy electrorefining experiments performed by Toshiba was also performed. LiCl-KCl-ZrCl4-ZrF salt was used and the process temperature was 650°C. The purpose of the experiment was to separate the radioactive species Co-60 from zirconium. Experimental results show that the DF for the electrodeposited Co can be obtained as 200/Step. As a result, the decontamination coefficient of 40000 was obtained. These results show that the process through electrorefiing can achieve a higher decontamination coefficient than the 1-step electrorefinig process through the 2-step process.

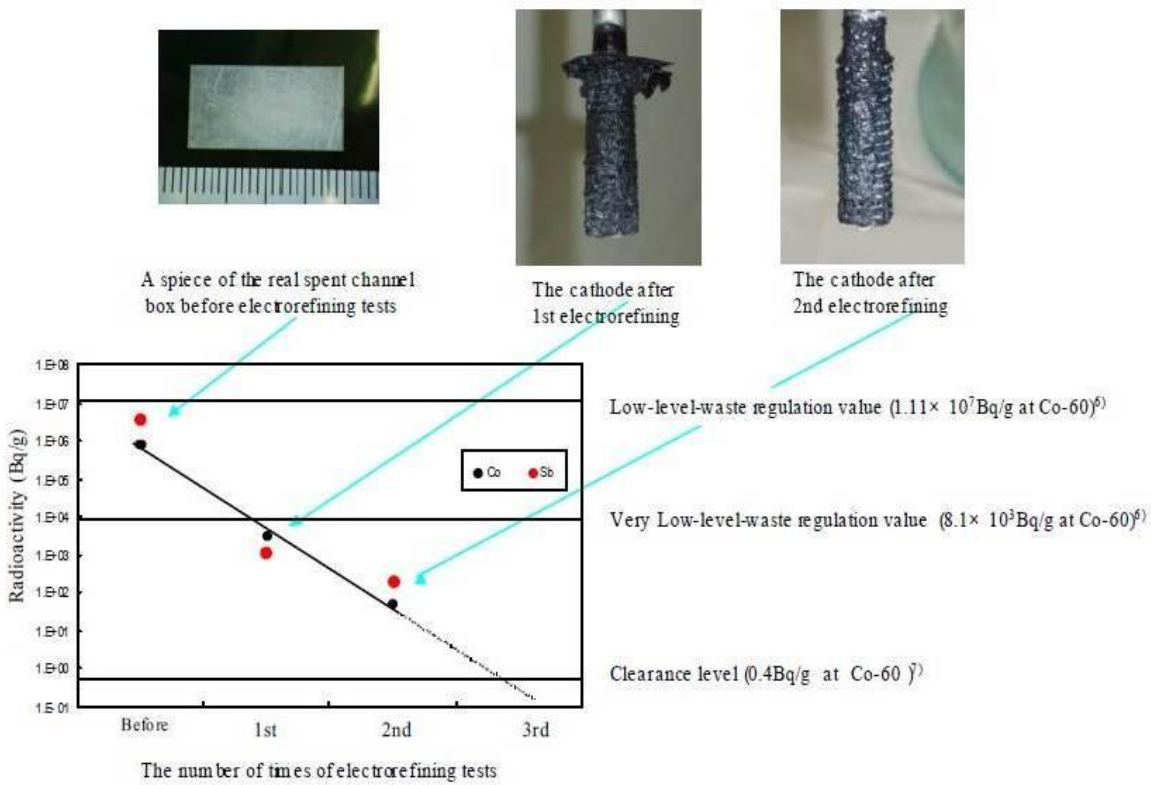

Figure 2.3 The results of electrorefining two step in LiCl-KCl-LiF

2.2.3 Electrorefining in Chloride salts

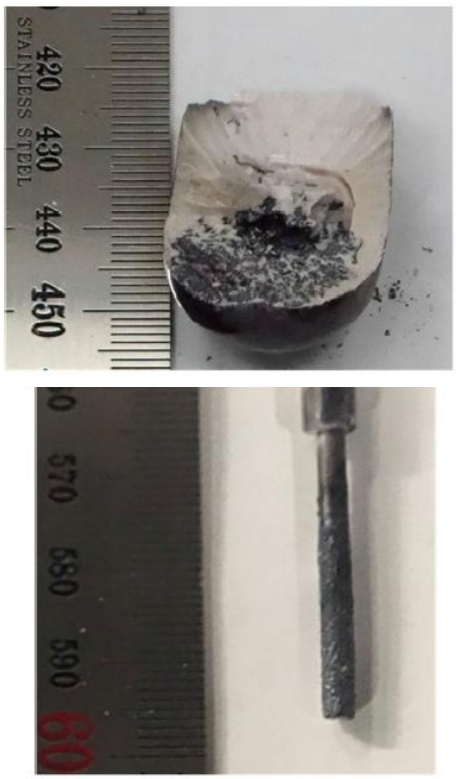

Figure 2.4 Deposited Zr on salt and cathode (J.Y. Park et al.)

Table 2.2 Composition of deposited Zr on cathode owith LiCl-KCl-$ZrCl_4$(J.Y. Park et al.)

	Zr-alloy Comp. (wt%)	Deposited concentration	DF
Zr	98.6	Over 99.999	-
Cr	1.104	N/D (<1ppb)	>552000
Sn	0.0830	N/D (<1ppb)	>41500
Fe	0.1595	N/D (<1ppb)	>79750
Co	0.0016	N/D (<1ppb)	>800

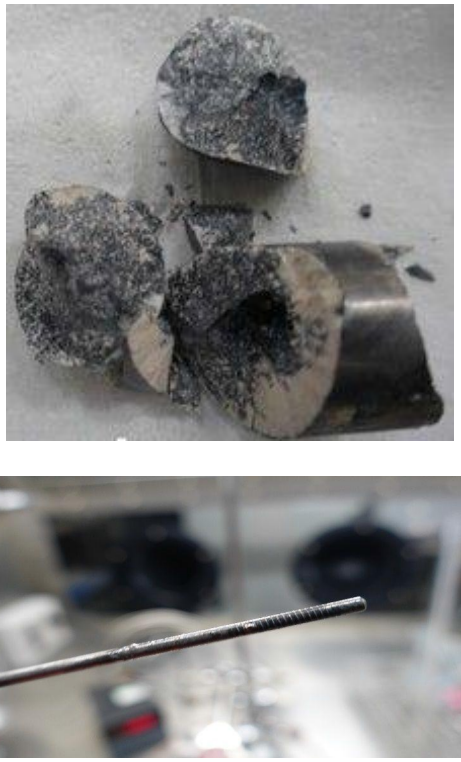

Figure 2.5 Deposited Zr on salt and cathode (P. H. Kim et al.)

Table 2.3 Composition of deposited Zr on cathode owith LiCl-KCl-$ZrCl_4$(P. H. Kim et al.)

	Zr-alloy Comp. (wt%)	Deposited concentration (ppm)	DF
Zr	98.093	Bal.	-
Nb	1.623	3.5 ~ 2.1	489 ~ 800
Ni	< 0.284	N/D (<0.02ppm)	-
Co	< 0.284	3.82	-

According to previous studies, chlorinated salts have a disproportionate reaction to the reduction of Zr metal. This disproportionate reaction is problematic when the zirconium metal is electrodeposited on the cathode during zirconium decontamination using electrorefining. Park (SNU) conducted an electrorefining process experiments on chloride salts. Zircaloy-4 was used as an anode. The process temperature was 500°C and the salt was LiCl-KCl-$ZrCl_4$. Experimental results showed that the zirconium metal with a very high purity of 99.999% or more was electrodeposited on the cathode and obtained a very high decontamination factor for various elements. These results confirmed the possibility of achieving Zirconium-Niobium separation through chloride salt.

Also, Kim P.H. (2016) performed an electrorefining process experiments using a Zr-Nb alloy (Hana cladding). LiCl-KCl-ZrCl4 salt was used and the process temperature was 500 ° C. As a result, the decontamination factor of 589 ~ 7100 was obtained, and the possibility of separation of Zirconium-Niobium by electrorefining was confirmed.

		Pros.	Cons.	Rank
Surface decontamination	Hydrofluoric acid process	• Simple process	• High Decontamination factor can't be obtained.	4
Volume decontamination	Iodination process	• High decontamination factor	• Deconposition process requires long reaction time • ZrI_4 is very hygroscopic	3
	Electrorefining in fluoride(-chloride) salts	• One step reduction metal deposition • Coarse metal recovery	• High operating remperature(650°C~800°C) • Fluoride corrosion • Complicated salt purification(for fluoride-chloride salt)	2
	Electrorefining in chloride salts	• Low operating temperature(500°C) • Low corrosion problem	• Complicated redox reactions • Disproportionate reaction • ZrCl deposition	1

Table 2.4 Comparison of each decontamination process for zircaloy

Table 2.4 summarizes the advantages and disadvantages of each process according to the results of previous research.

Considering the possibility of decontamination, safety, and economics, the electrorefining process is considered to be the most appropriate process.

Despite the advantages of the one-step reduction reaction in fluoride salt, the chloride electrorefining process is considered to be more safe than the fluoride electrorefining process in the commercialized size process.

Chapter 3 Rationale and Approach

3.1 Rationale and Research Goal

From the literature review, by electrorefining using chloride molten salt has been chosen the best separation process for zircaloys. Electrorefining with chloride molten salt has superior safety and efficiency compared to other separation process.

The main goal of this dissertation is to demonstrate high decontamination factor for Zr-Nb based on electrorefining in LiCl-KCl-$ZrCl_4$. To determine this, Zr and Nb redox reactions in LiCl-KCl molten salt must be studied. With various experiments, the thermodynamic data of zirconium and niobium can be determined and validated.

With this database, the electrorefining experiments can be simulated by 1-D code electrorefining model(REFIN). Then the electrorefining test should be made in lab-scale with model verifications. Finally, issues with cell design can be identified and overcame by engineering design. Then, this dissertation will address these specific questions defined as follows:

1. **Check the decontamination possibility of Nb, Co, Ni from Zr-Nb alloys by using electrorefining in LiCl-KCl eutectic molten salts**
2. **For lab-scale, determination experiment of Decontamination Factor(DF) on Nb**
3. **Design and pilot-sclae electrorefining cell for Zr-Nb separation**

3.2 Research approach

With eariler studies and ORIGEN-2 calculation, The target decontamination factor for Nb was set at 100,000. As a result of the previous research, electrorefining using chloride salt was adopted as the most efficient method of Zr decontamination. Accordingly, for electrorefining, thermodynamic data are collected by performing cyclic voltammetry to confirm the redox behavior of Zr and Nb in the LiCl-KCl salt.

Using the results, electrorefining calculation through 1-D simulation and electrorefining experiment on lab-scale are performed to demonstrate the possibility of separation of Zirconium-Niobium.

In addition, particles of Nb remaining on the cathode during electrorefining with the actual rotator may be deposited on the electrodeposited Zr metal. In addition, the ohmic drop problem caused by the installation of the basket to prevent Nb particle can greatly lower the efficiency of the electrolytic refining. Therefore, we solve two problems by using CFD (ANSYS-CFX) tool to solve the problems that may occur when cell design for electro refining.

In addition, the feasibility of the process is confirmed through the economic evaluation and comparison of the disposal of intermediate level wastes and the disposal of low-level wastes through decontamination processes in order to obtain the validity of the Zr electrorefining process.

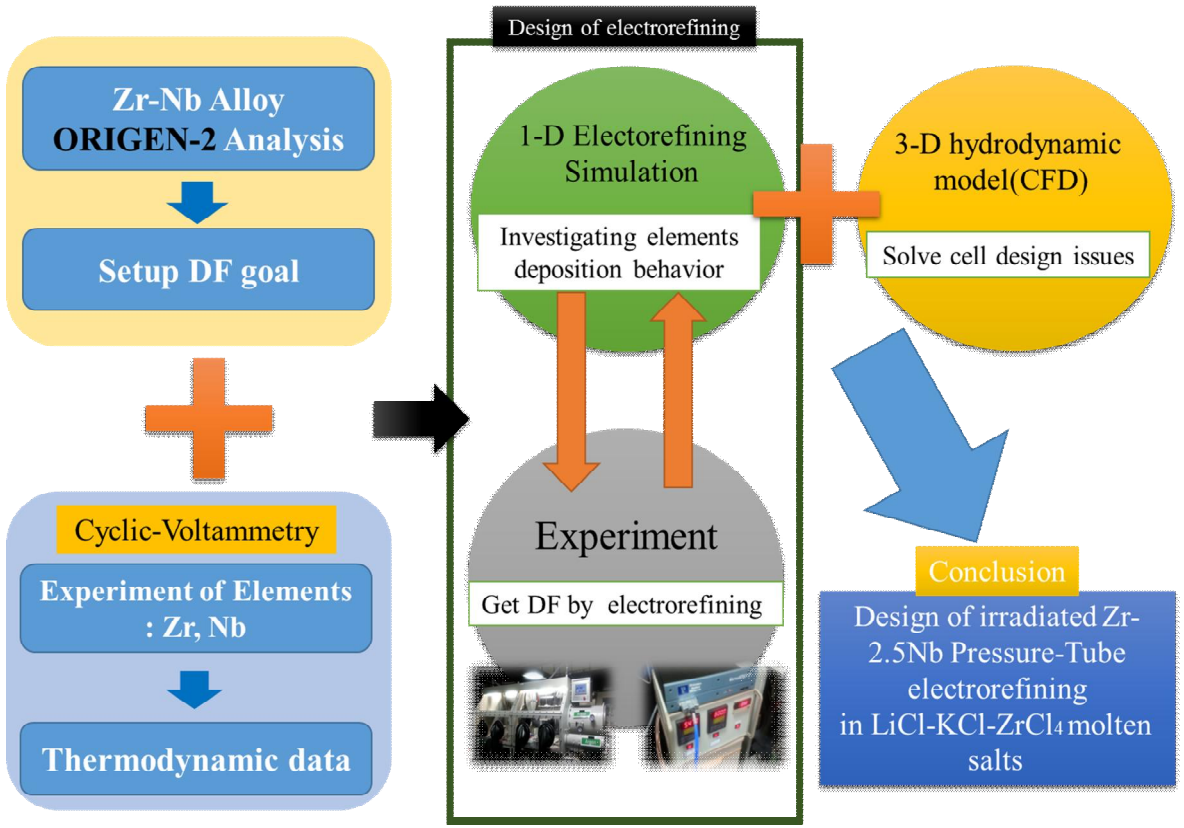

Figure 3.1 Schematic diagram for this thesis flow chart

Chapter 4 Electrochemical Experiments

Cyclic voltammetry (CV) is a method commonly used to identify the behavior of ions in electrolytes. In this study, the electrolytic behavior and thermodynamic data for Zr and Nb is also obtained using CV for LiCl-KCl-$ZrCl_4$ and LiCl-KCl-$NbCl_5$ salts

4.1 Materials and Apparatus

To check zirconium and niobium redox behaviors in LiCl-KCl eutectic salt, several cyclic voltammetry(CV) experiments were conducted. A glove box was filled and continually purged with inert argon gas of 99.999% by weight purity throughout experiments. Oxygen and moisture concentration was maintained below 0.1ppm and monitored during experiments. The working electrode(WE) and counter electrode(CE) material is 99.99 wt.% purity tungsten wire with 1mm diameter, 40cm length and smooth surface manufactured by Sigma Aldrich. The reference electrode was Ag/AgCl electrode containing 99.999% purity of Ag electrode with 1mm diameter and 1 wt% of AgCl salt manufactured by Sigma Aldrich. The purity of $ZrCl_4$ is 99.99 wt% manufactured by Sigma Aldrich. The purity of $NbCl_5$ is 99.9 wt% manufactured by Alfa Aesar. The molten salt mass for each CV experiment is about 3.0g, and WE and CE area for each CV experiment was about 0.628cm^2. The experiment temperature was 500±1°C.

Figure 4.1 Glove box used for experiments

Figure 4.2 Heat geneartor used for experiments

Table 4.1 Material purity and manufacturer for experiments

Material	Purity	Manufacturer
$ZrCl_4$	99.99%	Sigma-Aldrich
$NbCl_5$	99.9%	Alfa Aesar
LiCl-KCl	99.99%	Sigma-Aldrich

Table 4.2 Geometry and material for cyclic voltammetry

	Material	Area
Anode	W	$0.628cm^2$
Cathode	W	$0.628cm^2$
Ref. Electrode	Ag/AgCl(1wt%)	-
Molten Salt	LiCl-KCl	-

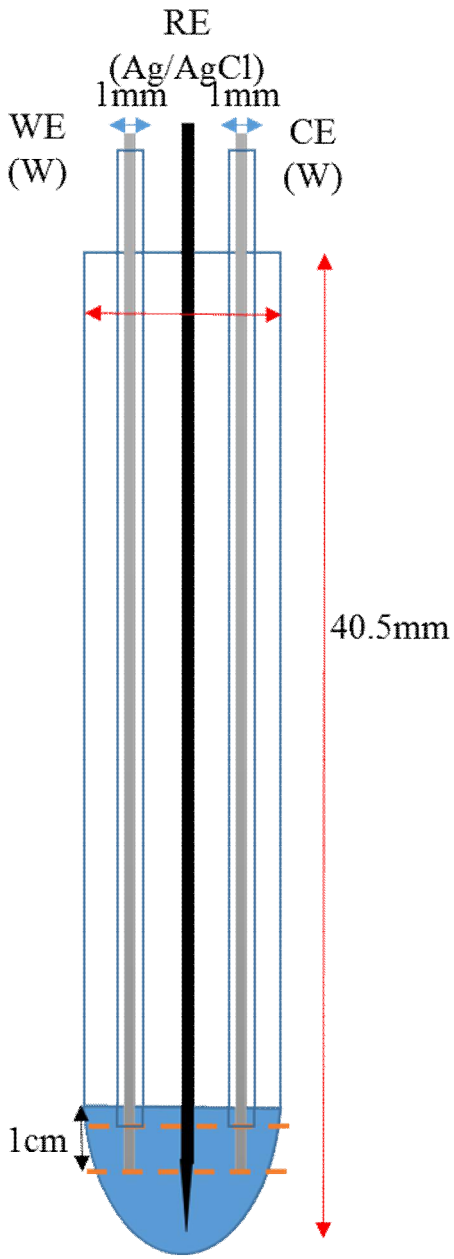

Figure 4.3 Schematic cell design for cyclic voltammetry experiments

Table 4.3 CV experiments table

Salt	Composition	Object
$LiCl$-KCl-$ZrCl_4$	$ZrCl_4$: 3.35wt%	- High composition Thermodynamic data
	$ZrCl_4$: 0.8wt%	- Low composition Thermodynamic data
	$ZrCl_4$: 1wt%	- Comparison with mixed salt - Oxidation reaction Potential
$LiCl$-KCl-$NbCl_5$	$NbCl_5$: 0 .32wt%	- Thermodynamic data
$LiCl$-KCl-$ZrCl_4$-$NbCl_5$	$ZrCl_4$: 1wt%, $NbCl_5$: 0.05wt%	- Thermodynamic data - Confirm about under mixed condition

4.2. Cyclic voltammetry of Zr and Nb in LiCl-KCl

4.2.1 Cyclic voltammetry of Zr in LiCl-KCl

To detect zirconium behaviors in LiCl-KCl, CV experiments were conducted. LiCl-KCl-$ZrCl_4$(1wt%, 0.8wt% of $ZrCl_4$) was prepared and conducted CV experiment.

Figure 1. is the result of LiCl-KCl-$ZrCl_4$ with scan range from -1.3V to 1.0V (vs. 1 wt% Ag/AgCl). It is well known by previous studies that the oxidation peak O_1 about -0.8V (vs. 1 wt% Ag/AgCl) reaction is the Zr metal is transformed to Zr(II) ion or Zr(IV). The reduction peak R_1 about -1.2V (vs. 1 wt% Ag/AgCl) is well know that from Zr(IV), Zr(II) to Zr(0) or Zr(I). It was detected that in the scan range from 0 to 1.0, there are no unusual redox peak was detected.

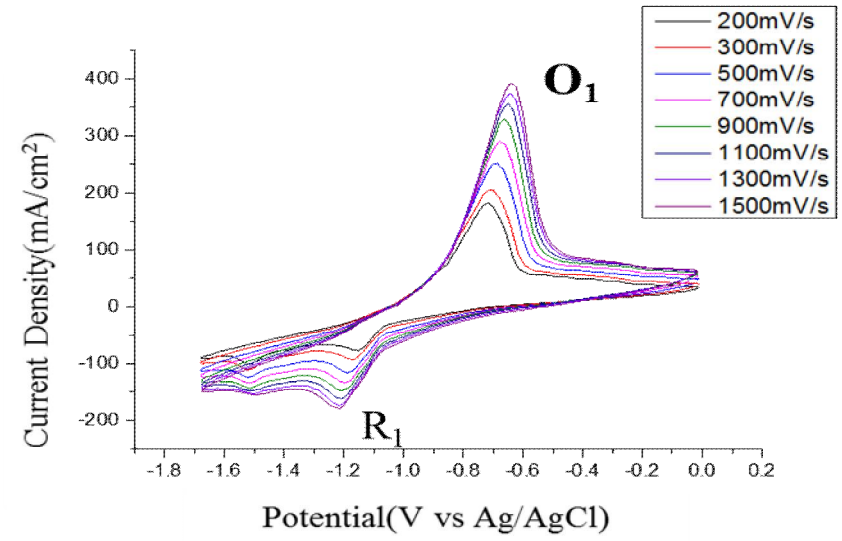

Figure 4.4 Cyclic voltammetry scan rate from 0 to – 1.7V (vs. 1 wt. % Ag/AgCl) 500°C LiCl-KCl-ZrCl4(0.8 wt. %)

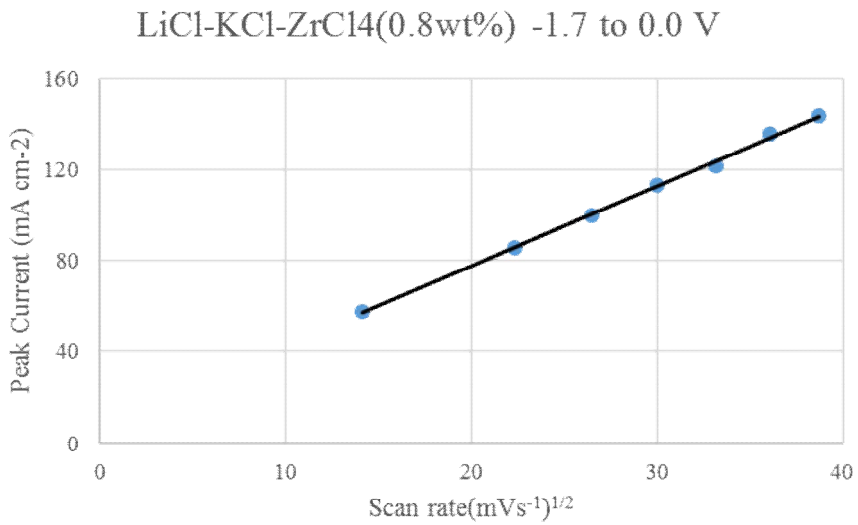

Figure 4.5 Linearity confirmation peak current vs scan rate

4.2.2 Cyclic voltammetry of Nb in LiCl-KCl

To detect Niobium behaviors in LiCl-KCl, CV experiment was conducted. LiCl-KCl-NbCl5(0.32wt%) was prepared and conducted CV experiment. And, other properties was same with Zr CV case.

Figure 1. is the result of LiCl-KCl-NbCl5 with scan range (-1.3V ~ 1.0V). It is also well know that the oxidation peak O2 about 0.2V (vs Ag/AgCl) is lowest niobium metal oxidation peak to Nb(III). And, The reduction peak R1 about -0.5V (vs Ag/AgCl) is well know that highest reduction peak from niobium ion (Nb(III)) to niobium metal(Nb(0)).

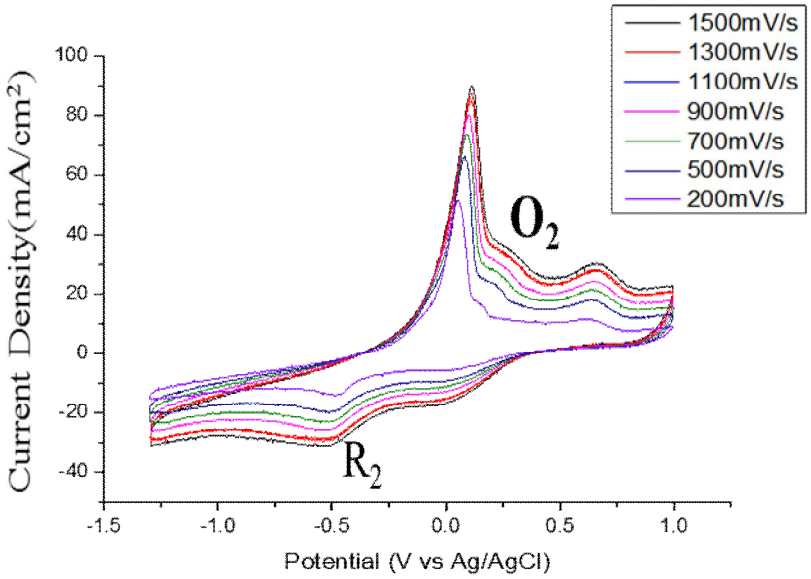

Figure 4.6 Cyclic voltammetry result of Zr in LiCl-KCl-$NbCl_5$ (0.32wt.% of $NbCl_5$) with scan range from -1.3V to 1.0V (vs. 1 wt% Ag/AgCl) with W electrodes at 500°C

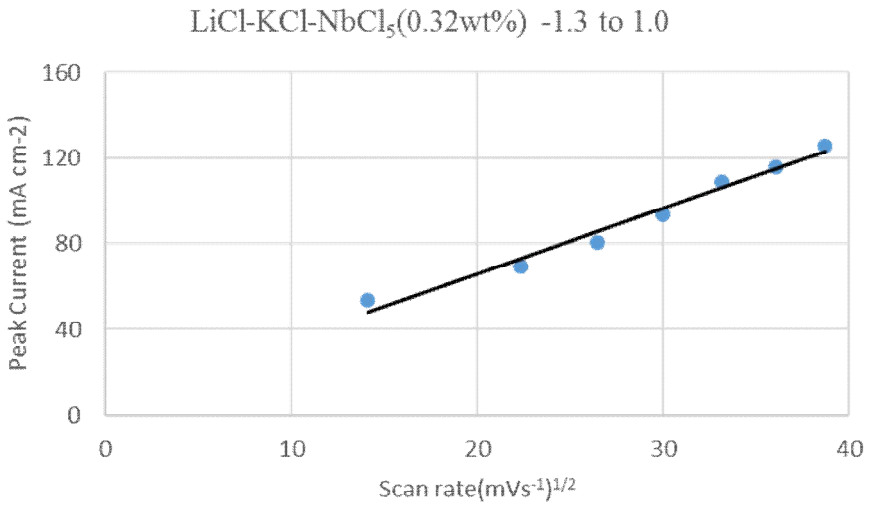

Figure 4.7 Linearity confirmation peak current vs scan rate

4.3. Cyclic voltammetry of Zr and Nb in LiCl-KCl-$ZrCl_4$-$NbCl_5$

Until now, there have been numerous CV experiments studies on LiCl-KCl salts including Zr salt or Nb salt. But, no experiment involving both Zr and Nb salts has been performed. Since the pressure tube contains both Zr and Nb metal, to confirm unusual redox reaction under Zr ion and Nb ion mixed condition, LiCl-KCl-$ZrCl_4$(1 wt%)-$NbCl_5$(0.1 wt%) salt was prepared and CV experiment was conducted.

Figure 3. is the CV experiment result of LiCl-KCl $ZrCl_4$(1 wt%)-$NbCl_5$(0.1 wt%) salt. From this result, O_1, O_2, R_1, R_2 redox peak was confirmed. Other unusual peak was not detected from this CV result.

These cyclic voltammetry redox peak shows that the metal oxidation peak difference is about 1.0V. This means electrorefining process is suitable for Zr-Nb separation.

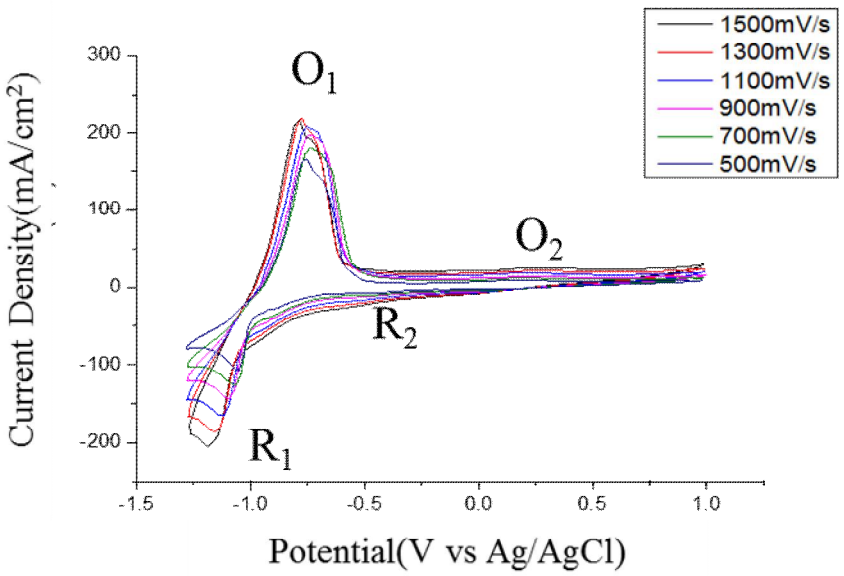

Figure 4.8 Cyclic voltammetry result of Zr and Nb in LiCl-KCl-$ZrCl_4$ (1 wt%)-$NbCl_5$(0.1 wt%) with scan range from -1.3V to 1.0V (vs. 1 wt% Ag/AgCl) with W electrodes at 500°C

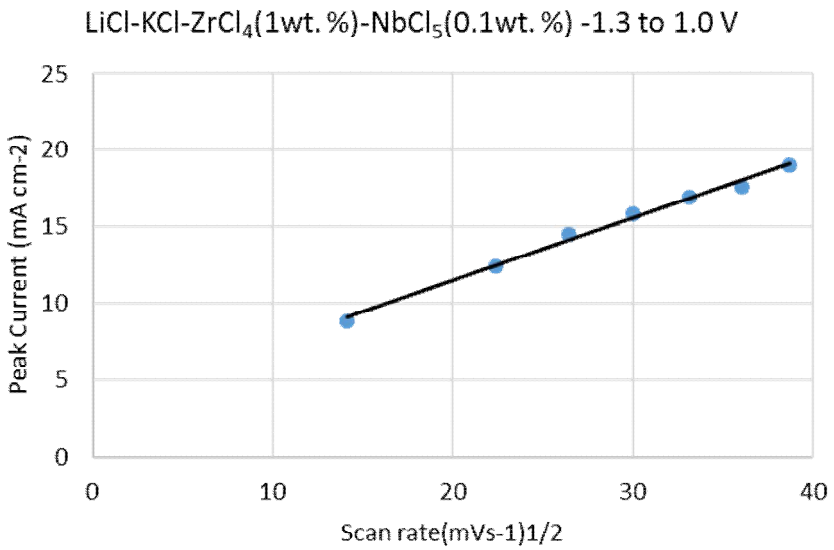

Figure 4.9 Linearity confirmation peak current vs scan rate

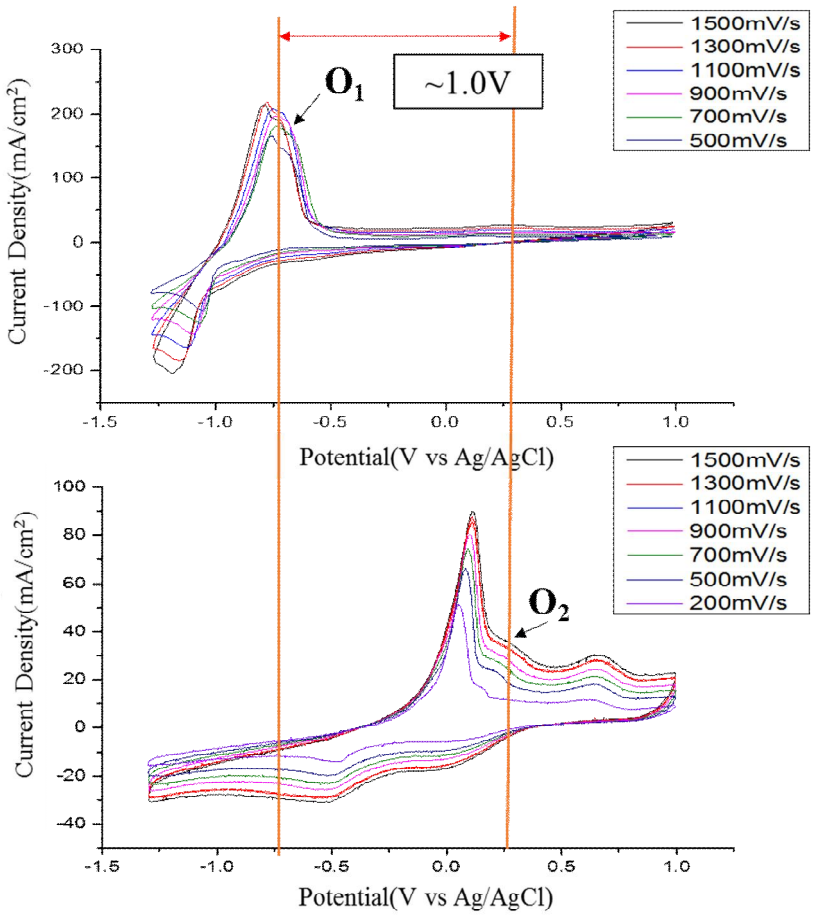

Figure 4.10 Oxidation peak difference for each elements(Zr and Nb) by cyclic voltammetry

4.4 Reduction of Thermodynamic data

From cyclic voltammetry data, diffusion coefficient and apparent equilibrium potential can be calculated.

4.4.1 Diffusion Coefficient

It is revealed that Zr(IV) is irreversible during cyclic voltammetry on cathodic reaction R_1.

$$\frac{I_{pc}}{\sqrt{v}} = -0.4958nFSC\sqrt{\frac{n\alpha FD_{ox}}{RT}}$$

Above equation is Delahay equation calculating diffusion coefficient for irreversible reaction. n is the number of electrons participating in the reaction, F is the Faraday's constant (96.485 C/mol), R is the universal gas constant (8.314K/mol/K), v is scan rate, I_{pc} is peak current, α is transfer coefficient, it is generally assumed as 0.5, T is the temperature.

$$i_p = 0.446(nF)^{3/2}C\left(\frac{Dv}{RT}\right)^{1/2}$$

Above equation is the equation for reverssible equation. C_{M+} is the concentration of metal ion.

Zirconium and Niobium diffusion coefficient data is shown as from Table 4.4 and 4.5 It is reliable with other previous experiment data.

4.4.2 Apparent Equilibrium Potential

From cyclic voltammetry data, apparent equilibrium potential can be obtained. Zirconium is irreversible during cyclic voltammetry on cathodic reaction R_1

$$E_{pc} = E^{0*} - \frac{RT}{\alpha nF}[0.78 - \ln k_s + \ln(\sqrt{\frac{\alpha nF\nu D_{OX}}{RT}})]$$

Equation (3) is Delahay equation calculating standard reduction potential for irreversible reaction. E_p is the peak potential.

$$E_p = E^{0\prime} + \frac{RT}{nF}\ln C_{M^{n+}} + 0.8540\frac{RT}{nF}$$

Above equation is the equation for reverssible equation. Niobium is reverssible on Cathodic reaction R_2.

Zirconium and Niobium apparent equilibrium potential data is shown as from Table 4.6 and 4.7. It is reliable with other previous experiment data.

Table 4.4 Diffusion coefficient of Zr in LiCl-KCl

Salt composition	Diffusion Coefficient (*E-05cm^2/sec)	Diffusion Coefficient (*E-05cm^2/sec)
$ZrCl_4$ =0.8 wt%	1.660 ± 0.040	1.681 ± 0.231
$ZrCl_4$ =1.0 wt%	1.925 ± 0.315	
$ZrCl_4$ = 1.0wt% $NbCl_5$ = 0.1wt%	1.460±0.160	

Table 4.5 Diffusion coefficient of Nb in LiCl-KCl

Salt composition	Diffusion Coefficient (*E-06cm^2/sec)	Diffusion Coefficient (*E-06cm^2/sec)
$NbCl_5$ = 0. 32wt%	1.131±0.257	1.690
$ZrCl_4$ = 1.0wt% Nb = 0.1wt%	3.329	

Table 4.6 Appaerent equilibrium potential of Zr in LiCl-KCl

Salt composition	Redox Potential (V vs Ag/AgCl)	Total Average Potential (V vs Ag/AgCl)
$ZrCl_4$ = 3. 35 wt%	-1.134±0.021	-1.098±0.023
$ZrCl_4$ = 0.8 wt%		
$ZrCl_4$ = 1.0 wt%	-1.101±0.012	
$ZrCl_4$ = 1.0wt% $NbCl_5$ = 0.1wt%	-1.021±0.051	

Table 4.7 Appaerent equilibrium potential of Nb in LiCl-KCl

Salt composition	Redox Potential (V vs Ag/AgCl)	Total Average Potential (V vs Ag/AgCl)
$NbCl_5$0.32wt%	-0.422±0.02	-0.407±0.015
$ZrCl_4$ 1.0wt% $NbCl_5$ 0.1wt%	-0.393±0.02	

Chapter 5 Electrorefining studies

5.1. 1-D simulation

$$i = i_0 \cdot \left[\exp\left(\frac{\alpha_A nF}{RT} \eta \right) - \exp\left(-\frac{\alpha_C nF}{RT} \eta \right) \right]$$

REFIN, an electrorefining calculation tool developed by Seoul National University, performs a 1-D simulation using the butler-volmer equation. The diffusion coefficient and apparent equilibrium potential, which are thermodynamic data obtained from the previous CV, are used as inputs. Based on these results, we confirm the behavior of electrorefining of zircaloy internal elements over time and design the electrorefining method.

5.1.1 Benchmark Problem

A benchmark was performed to validate REFIN before simulation of electrorefining using REFIN code.

At the University of Utah, the purify process of electrolytic salts was carried out through a galvanic reaction. It is an experiment to reduce salts by reducing U and Mg with LiCl-KCl-UCl_3-$MgCl_2$ salt using gadolinium rod.

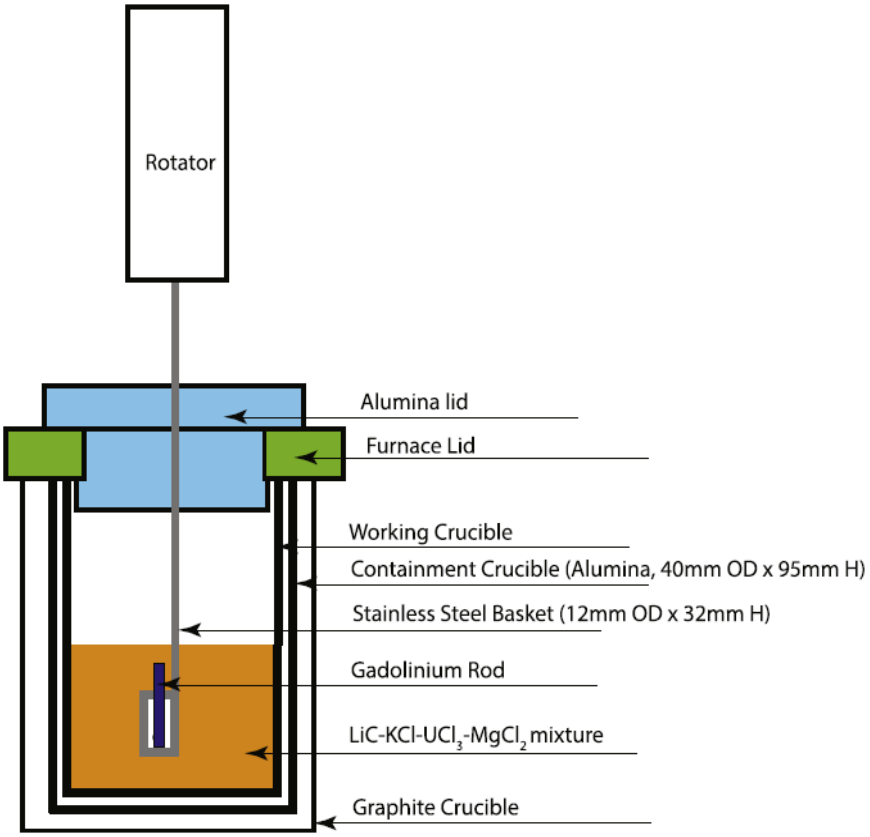

Figrue 5.1 schematic diagram of experiments benchmark problem

‘

Table 5.1 material appaaratus for benchmark problem

	Gadolinium Rod	Molten Salt
Mass(g)	7.96	47.33
Volume(cc)	1.01	29.22
Composition	99.9% gadolinium	LiCl-KCl -UCl_3(8.06wt%) -$MgCl_2$(1.33wt%)

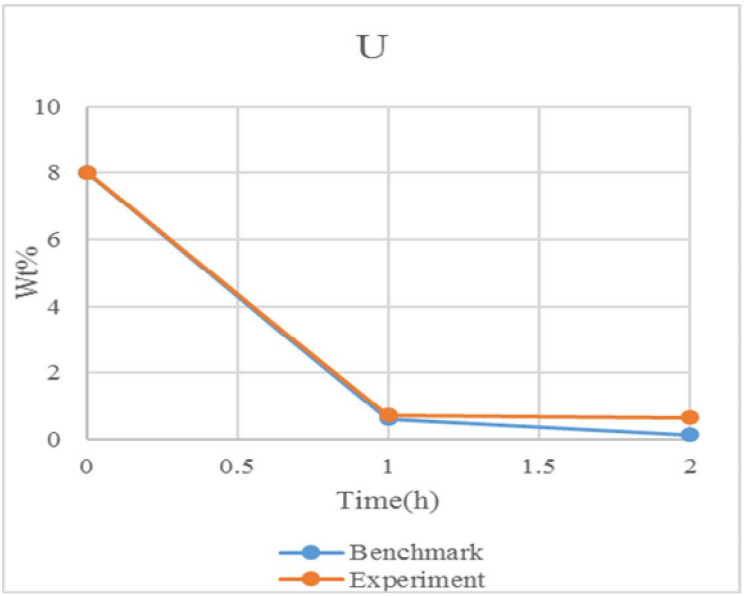

Figrue 5.2 UCl_3 compostion in salt comparison for benchmark and experiment

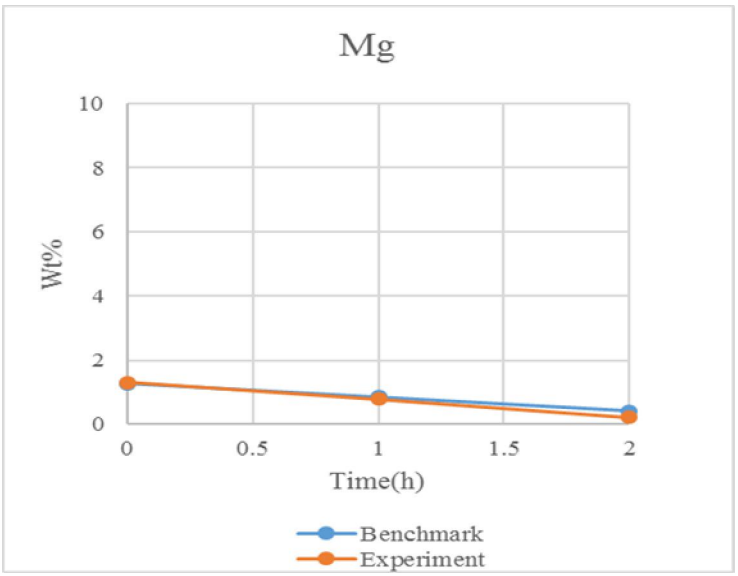

Figrue 5.3 $MgCl_2$ compostion in salt comparison for benchmark and experiment

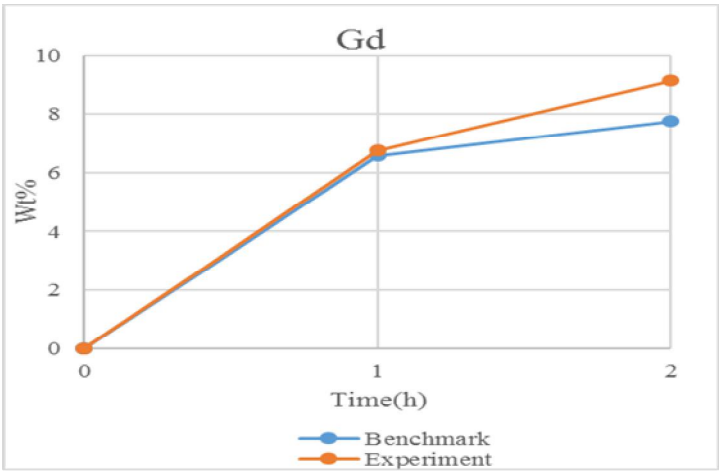

Figrue 5.4 $GdCl_3$ compostion in salt comparison for benchmark and experiment

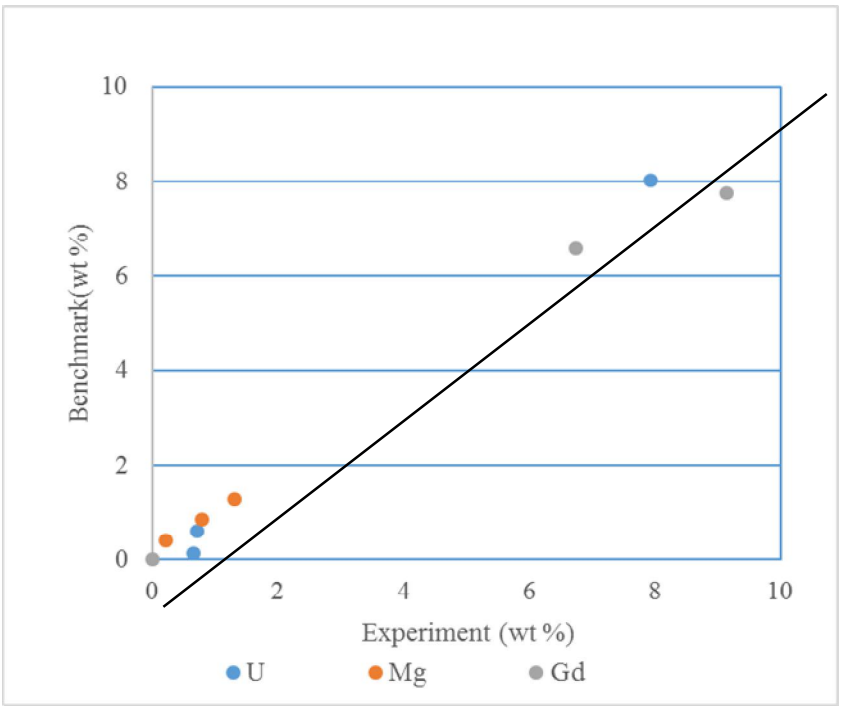

Figrue 5.5 Each element compostion in salt comparison for benchmark and experiment

Simulation results show that U and Mg are reduced in the salt. Simulation results for the total of 2 hours are shown in Figure 5.2, 5.3, 5.4 and 5.5 above. The behavior of each element during the experiment was found to be similar to that of the experiment, and a composition error of 20 ~ 30% was observed. The validation of the simulation of electrolytic refining process through REFIN was obtained from these results.

5.1.2 Zr-2.5Nb electrorefining 1-D simulation

The validation of REFIN was confirmed through the above benchmark results. 1-D simulation was performed to confirm the decontamination possibility of zirconium alloy through electrorefining process and to confirm the behavior of elements. This simulation does not take into account the problem of contamination of the particles coming from the anode, so we can see the most optimistic result of electrolytic process.

The speciation of the anode and salt for this simulation is shown in Figure 5.6 and Table 5.2, 5.3.

The geometry of the anode is assumed to be Zr-2.5Nb square, and CE is assumed to have a cylindrical shape and area and volume are set. The compositions of the anodes were obtained by cooling for 10 years after ORIGEN-2 30yr irradiation.

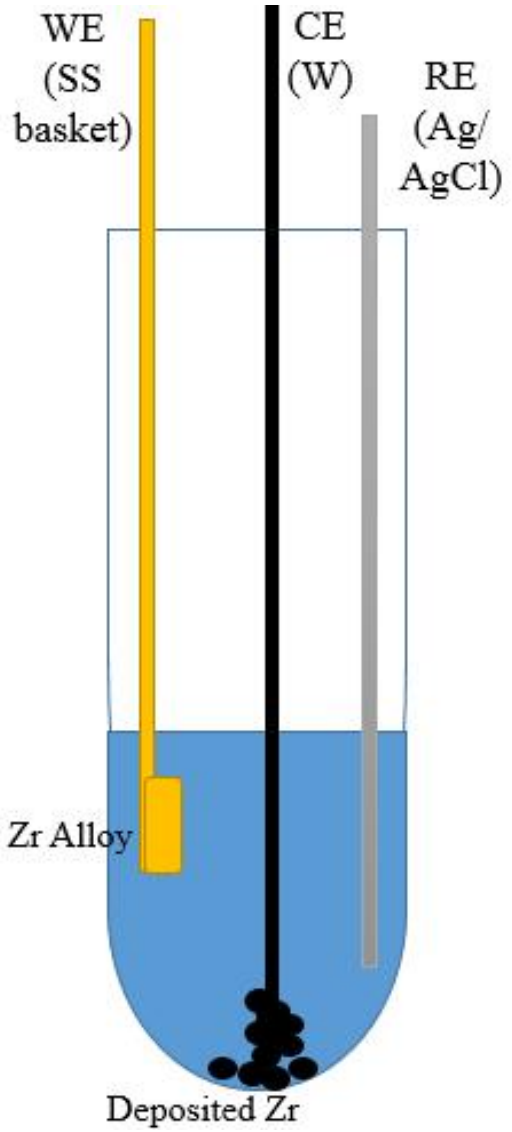

Figure 5.6 Cell design for 1-D simulation

Table 5.2 1-D simulation material apparatus

	Material	**Mass**
Anode	Zr-2.5Nb	3.14g
Molten Salt	LiCl-KCl-$ZrCl_4$(0.5wt%)	40g

Table 5.3 Anode composition for 1-D simulation

Element		**Initial Composition (wt%)**
-	**DF goal**	
Zr	**-**	**97.3**
Nb	**1E+05**	**2.46**
Fe	**-**	**>0.15**
Cr	**-**	**>0.01**
Co	**-**	**>0.01**
Ni	**-**	**>0.01**

Simulation results show that Zr, which has the lowest oxidation potential, is oxidized first, and Zr ions in the salt are first electrodeposited in metal form in the cathode. Over time, other remaining materials begin to deposit a little, and when the zirconium composition of the anode becomes very small, other elements including the Nb of the anode begin to rapidly deposit. Thereafter, Nb starts to electrodeposit. The electrolysis process must be stopped before this happens. The composition and DF of the electrodeposited zirconium when 99.9% zirconium was recovered from the anode were thus shown in Table 5.4. It is confirmed that the maximum DF of Nb can be obtained up to 4.84E+08 in REFIN 1-D simulation. These results confirmed the possibility of separation of Zirconium-Niobium through electrolytic refining and confirmed the behavior of the elements in the electrolytic process.

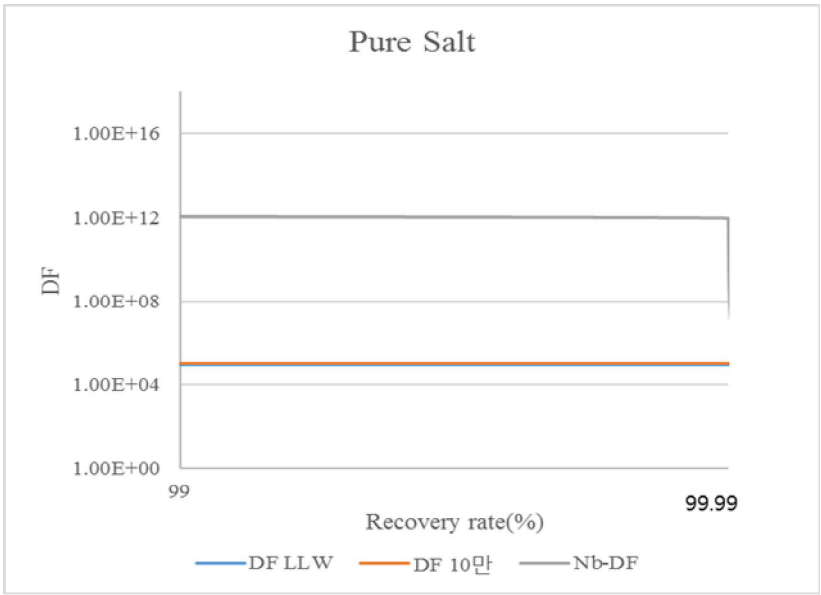

Figure 5.7 DF vs Zr recovery rate

Table 5.4 1-D simulation results at Zr 99.99% recovery rate.

Element	DF goal			Cathode Composition (wt%)		Salt Composition (wt%)	DF
	LLW	VLLW	EW				
Zr	-	-	-	>99.999		3.92E-02	-
Nb	8.0E+04	8.39.E+05	8.39.E+07	9.17E-10		4.28E-07	**4.84E+08**
Fe	-	4.18.E+01	4.18.E+03	1.59E-08		2.16E-07	9.49E+06
Cr	-	-	-	7.11E-07		7.83E-07	1.40E+04
Co	-	2.38.E+06	2.38.E+08	1.74E-12		1.11E-10	4.29E+08
Ni	-	1.26.E+02	1.26.E+04	6.20E-14		1.33E-11	1.35E+11
Recovery rate	-	-	-	-		>99.99%	

5.2. Electrorefining experiments

5.2.1. Experiment Setup

A glove box was filled and continually purged with inert argon gas of 99.999% by weight purity throughout experiments. Oxygen and moisture concentration was maintained below 0.1ppm with continuous monitoring during experiments. The working electrode(WE) and counter electrode(CE) material is 99.99 wt.% purity tungsten wire with 1mm diameter, 40cm length and smooth surface manufactured by Sigma Aldrich. The reference electrode was Ag/AgCl electrode containing 99.999% purity of Ag electrode with 1mm diameter and 1 wt% of AgCl salt manufactured by Sigma Aldrich. The purity of $ZrCl_4$ is 99.99 wt% manufactured by Sigma Aldrich.

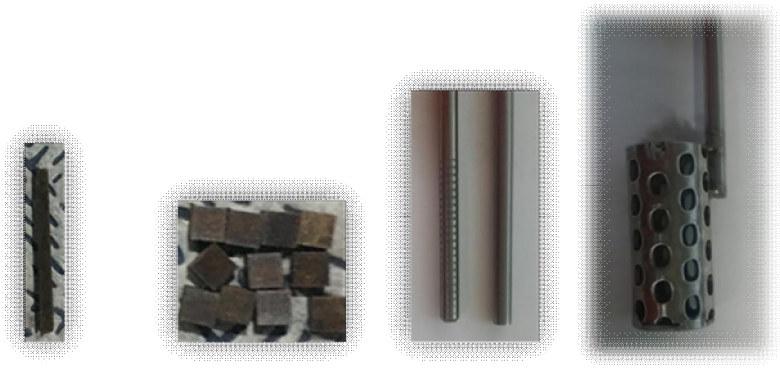

Figure 5.8 materials used for electrorefining experiments cell design (left : rod and chopped Zr-2.5Nb right : Tungsten rod and SS basket)

The main goal of the Electrorefining experiment is to separate Zirconium from Zr-2.5Nb. Since Nb has a positive oxidation potential compared to zirconium, it does not seem to dissolve when a certain voltage is applied to the anode. However, when it is dissolved in the electrolyte, it is expected to be electrodeposited in metal form before Zr due to positive reduction potential compared with Zr. Therefore, experiments were carried out to maintain the anode voltage constant, suppress the oxidation of Nb, and induce oxidation of Zr to recover pure zirconium.

In addition, in the experiment of P. H. Kim[Kim et al.], Nb was detected at the cathode despite the anode potential maintained at -0.85 V (vs Ag / 1 wt.% AgCl), and the decontamination factor could not be obtained by the 1-step process.

Since Nb is uniformly distributed in Zr, Zr is deposited on cathode and Nb particles are captured in the cell. In addition, the Zr electrodeposits of the precedent studies are unevenly distributed in the electrolyte due to the dispropotionate reaction. Therefore, to overcome the disadvantages of previous experiments, a basket is added to separate Nb and Zr, and designed an experimental cell to contain Zr salt in the basket.

Table 5.5 shows the lab-scale electrorefining experiments setup in this study. In experiments 1 and 2, an anode was installed outside the basket and Zr was collected in the basket. In the third experiment, an anode was installed in the basket to capture Zr outside the basket and to separate the Nb particles. These experiments were carried out using a potentiostatic electrorefining method with -0.9V (vs Ag / 1wt.% AgCl) applied to the anode. Molten salt used LiCl-KCl-$ZrCl_4$ (1 wt.%), Zr-2.5Nb for anodes and tungsten for cathodes.

	Experiment #1	Experiment #2	Experiment #3
Anode	Zr-2.5Nb rod		Chopped Zr-2.5Nb
Cathode	W rod (Φ1 mm)	W rod (Φ3.175 mm)	W rod (Φ1 mm)
Cell Design	Cathode : Al_2O_3	Cathode : Quartz	Anode : SS basekt & Quartz
	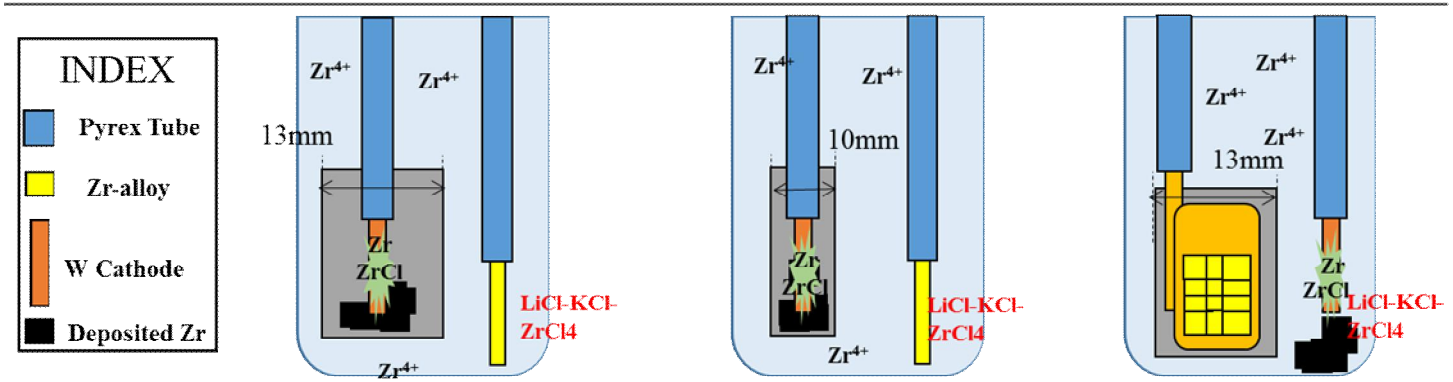		

Table 5.5 Experiments setups for lab-scale electorefiing

5.2.2 Electrorefining results of Zr-Nb alloys

Results of this experiment can be summarized as follows. The results shown in Figure 5.9 show that the salt was not electrodeposited well on the cathode in the previous experiment and that the ZrCl or Zr metals deposited on the bottom were unevenly distributed to lower the recovery rate and contaminate the salt and make it difficult to recover zirconium . In these experiments, deposited Zr were well distributed at the bottom of the basket as shown in Figure 5.10, confirming that the molten salts outside the basket were not contaminated. Through this, it was confirmed that Zr can be recovered effectively compared with the existing method, and it was confirmed that a basket was essential for the actual design of the electrorefining cell.

Figure 5.9 deposited Zr and salt after electrorefining in previous study
lower left and right : [Kim et al], upper left : [Park et al]

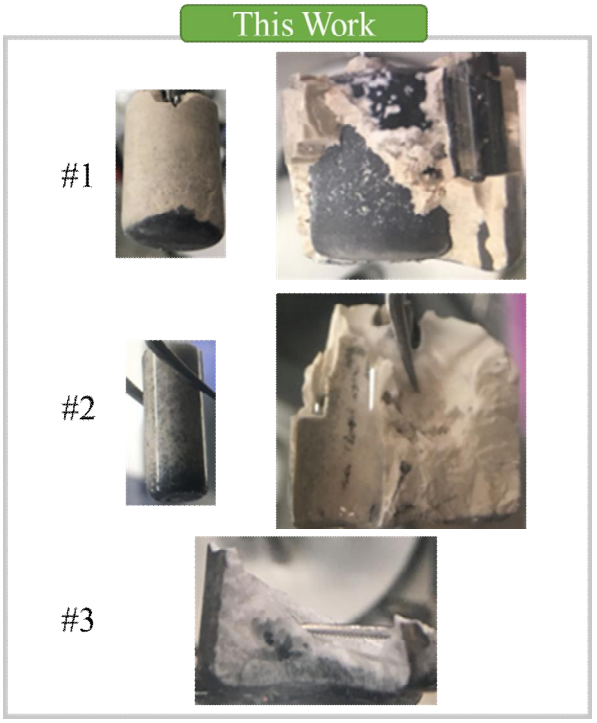

Figure 5.10 deposited Zr and salt after electrorefining in this study

In addition, diposited Zr settled on the bottom were measured by ICP MS and XRD.As a result of XRD analysis, it was revealed that chemical forms of deposited Zr in these experiments were Zr and ZrCl.

As a result of ICP-MS analysis, the composition of deposited Zr was measured. In this result, It was revealed that experiments #1 and #2 with showed lower DF cathode basket, 99.999wt.% of zirconium was deposited. In 3# experiments, with SS basket around anode, DF was measure to exceed 200,000. The experiment #3 value is greater than 100,000, the DF goal. This result means that decommissioned Zr-2.5Nb can be decontaminated to LLW by electrorefining in anode basket is installed. As shown in Fig 5.14, the anode basket can keep Nb particles from deposition on cathode.

Elements	Composition(ppm)	DF
Nb	0.24	1.03E+05
Fe	17.36	-
Co	0.15	133
Ni	23.22	-

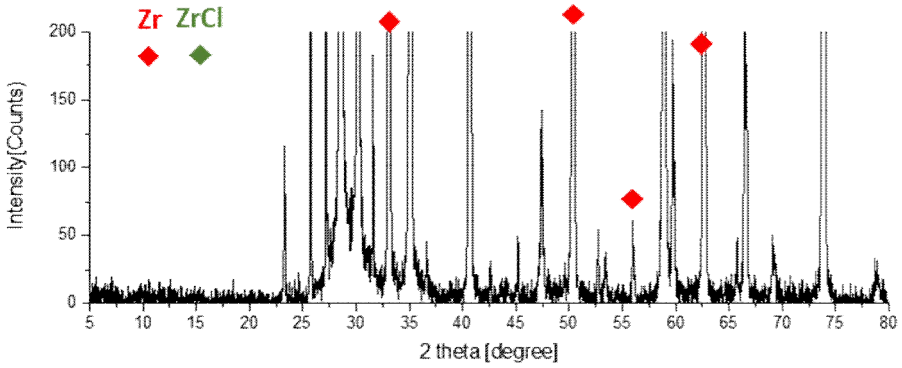

Figure 5.11 deposited Zr composition measred by ICP-MS and XRD measured data in experiment #1

Elements	Composition(ppm)	DF
Nb	1.26	1.21E+04
Fe	27.77	-
Co	0.03	666
Ni	14.05	-

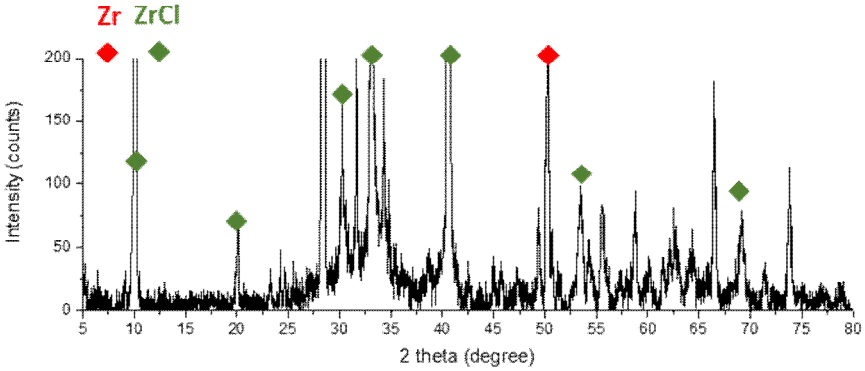

Figure 5.12 deposited Zr composition measred by ICP-MS and XRD measured data in experiment #2

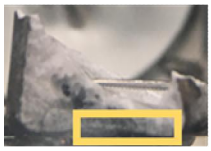

Elements	Composition(ppm)	DF
Nb	N/D<0.1	> 2E+05
Fe	12.01	-
Co	N/D<0.1	>1E+03
Ni	15.55	-

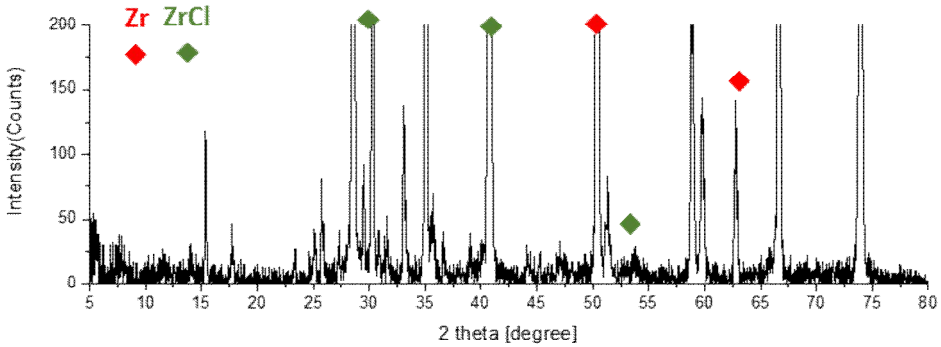

Figure 5.13 deposited Zr composition measred by ICP-MS and XRD measured data in experiment #3

	W/o basket(Ref.)	With cathode basket	With Anode Basket
Nb DF	489~7100	1E+04~05	>2E+05
Cell Design INDEX Pyrex Tube Zr-alloy W Cathode Deposited Zr	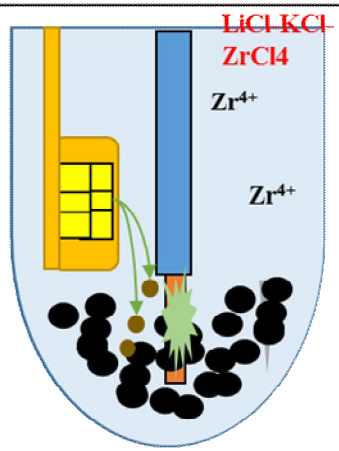	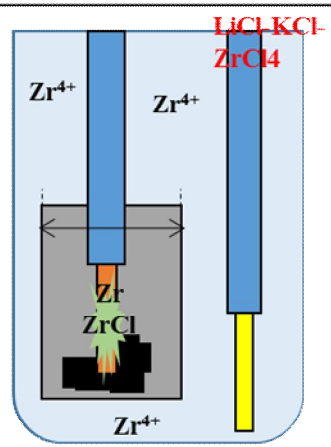	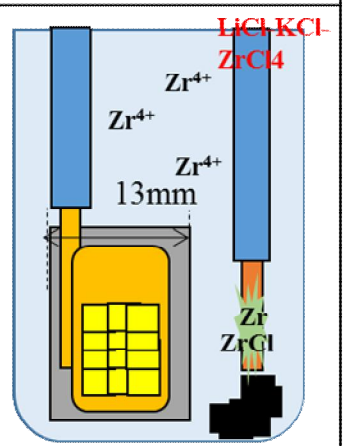

Figure 5.14 For each condition related to Nb particle effect control

5.3. Element Flow chart

Through the experimented studies, it was confirmed that the decontamination factor of Nb can reach the target value of 100,000 through the electrorefining process for the decommissioned Zr-2.5Nb. when anode basket is installed. As a result, a flow chart of each element in the decontamination process of electrorefining can be obtained. First, Zr electrodeposited on cathode or basket is classified as low-level waste because it contains weakly-radioisotope Zr-93. This Zr is consolidated as an ingot, disposed in the LLW repository, or used as a structual metals in nuclear supplements. In addition, Nb and C remaining in the anode after the electrorefining process are partially stored in the ILW interim storage, and additional decontamination is performed through final disposal or transmutation. In addition, the salts used in the electrorefining process can be partially contaminated by materials such as Nb. These salts can be recycled through zone refining process [PyroGreen white paper].

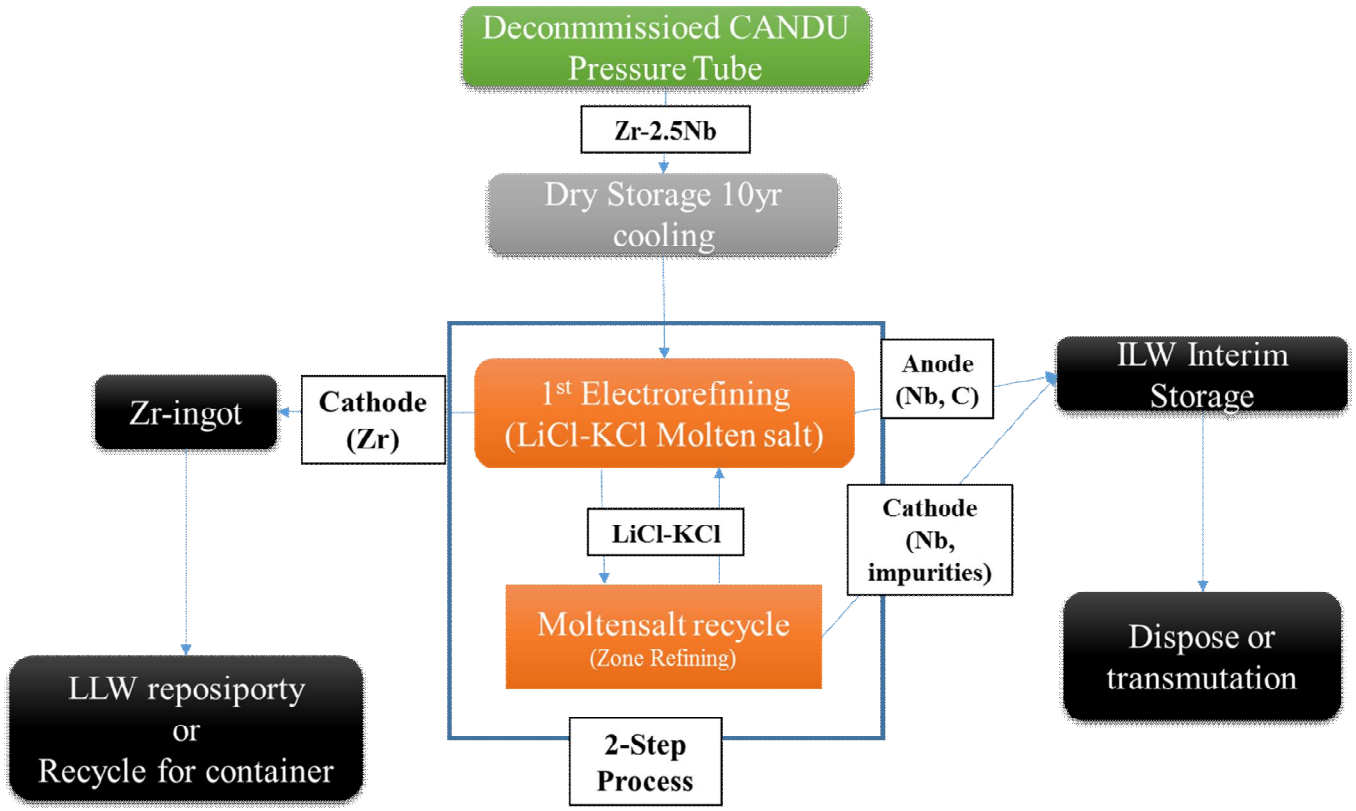

Figure 5.15 Element flow chart for electrorefining

6. Cell Design

6.1 Cell Design and Challenging Issue

6.1.1 Nb Droplet

Previously, we experimented and simulated electrorefining in lab-scale without any flow. However, in an actual pilot-scale or commercial scale process, the anode and cathode are rotated to reduce the diffusion layer to control the limiting current during the electrorefining process. In this case, a flow may occur in the fluid, and Zr and Nb droplets may penetrate into or leave the basket. Simulation was performed by rotating the electrodes of the previous experiment cell.

These are several assumptions for simulation.

1. Rotating Speed : 50rpm (Ref : Mark-IV)
2. Droplets diameter : 1e-06m (assumed)
3. Particle Tracking simulation time : 2000s
4. Drag force : Stoke's law

In this simulation, the amount of Nb particles from the anode entering the cathode basket was 44%. This means that Zr electrodeposited by Nb particles can be contaminated during electrorefining.

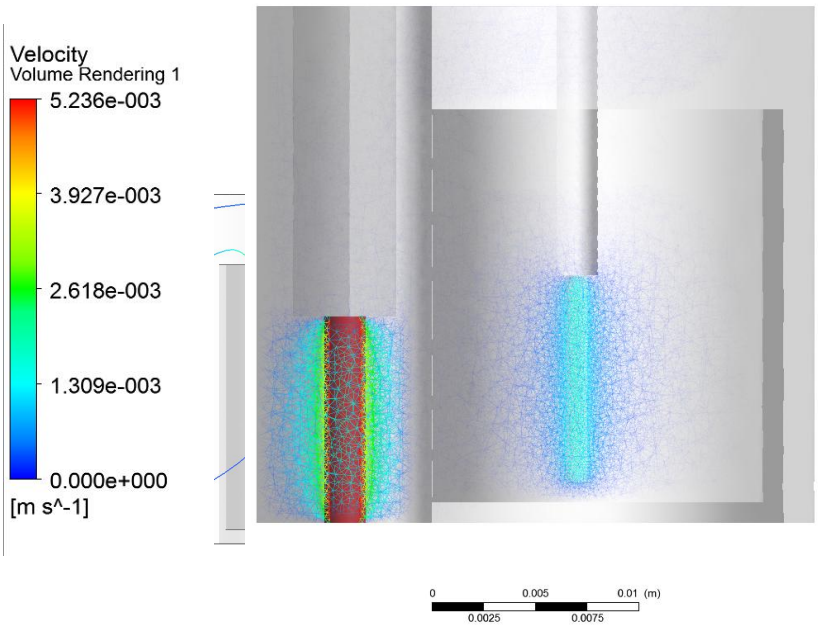

Figure 6.1 Flow velocity distribution around rotating electrodes

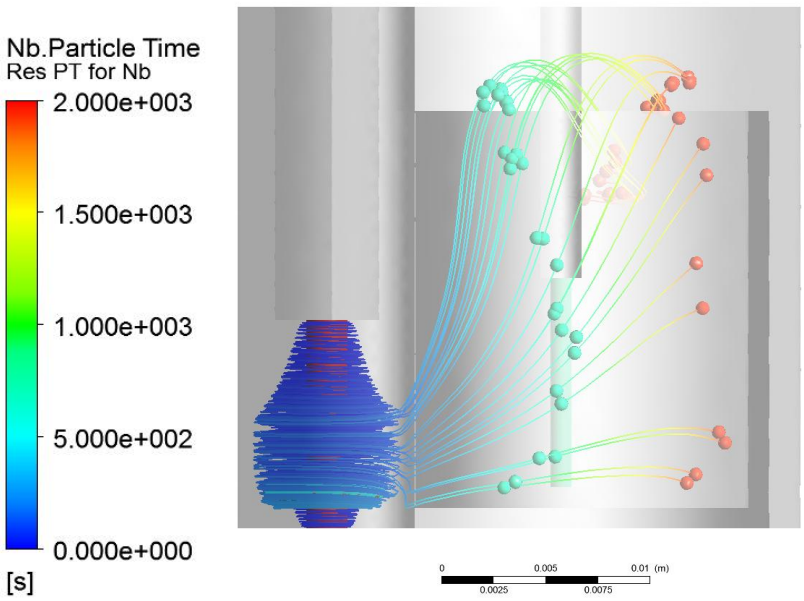

Figure 6.2 Nb particle tracking with flow velocity by rotating electrode

Table 6.1 particle tracking results with flow velocity

Elements	In the basket	Out of basket
Nb	44% (20/46)	56% (26/46)
Zr	100% (100/100)	0% (100/100)

6.1.2 Ohmic Drop

To prevent particles from entering the basket above, an effective method is to add a basket around the anode. However, in this case, the path in the electrolyte increases and the path from the anode to the cathode narrows, resulting in more ohmic drops. To overcome the disadvantage, a 3-D simulation is made by using ANSYS-CFX.

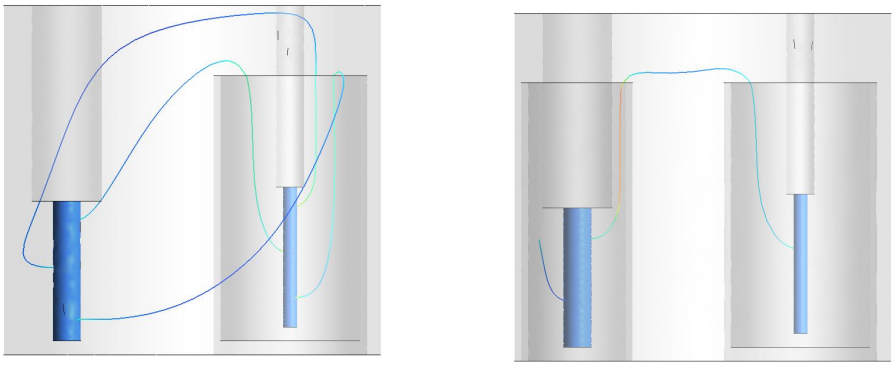

Figure 6.3 ohimc drop path (left : w/o basket, right : w/ basket)

These are several assumptions for simulation.

1. Applied current density : 0.1mA/cm2
2. Electrolyte conductivity : 187.22 (S/m)
3. Anode potential : 0 V

$$V = IR = I \times \rho \times \frac{L}{A}$$

I : Current density L : path length

ρ : resistivity A : path area

In this case, it was confirmed that the ohmic drop increased more than three times, when both anode basket and cathode basket we added. and it was confirmed that although the addition of the basket was indispensable, the efficiency was decreased.

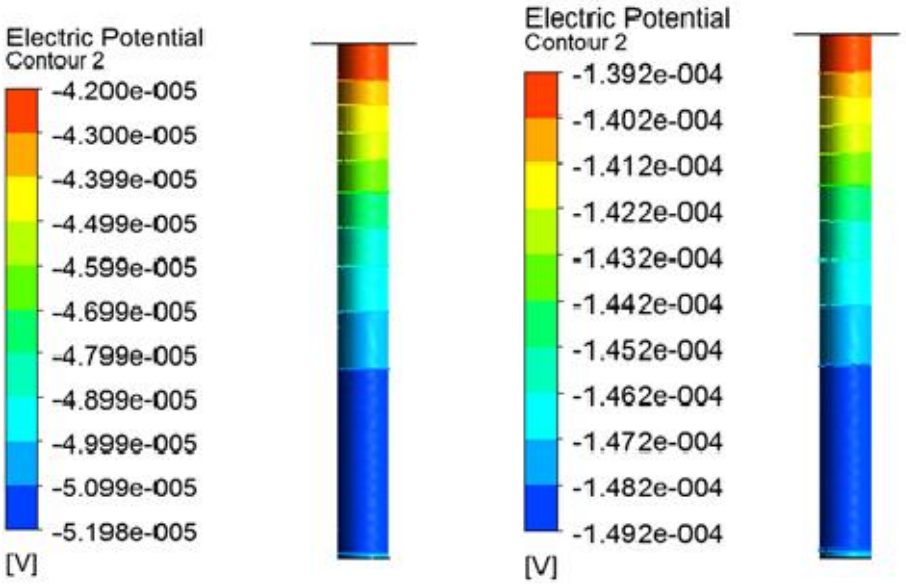

Figure 6.4 Potential distribution on cathode

(left : w/o basket right w/ basket)

Table 6.2 Ohmic drop comparison within this simulation

Index	w/o wall	w/ wall
Lowest Potential(V)	-4.200e-05	-1.492e-04
Highest Potential(V)	-5.198e-05	-1.392e-04

6.2 New design cell

As a method to solve the Nb droplet intrusion and ohmic drop issues discussed above, the cell was designed by adding holes to the basket. In this case, it was confirmed that the ohmic drop increased by a factor of three times. It was confirmed that the current flow around the anode basket did not occur, and the particle tracking simulation showed that the particle did not penetrate into the cathode basket. Therefore, in the cell design hole were added around the anode and cathode baskets.

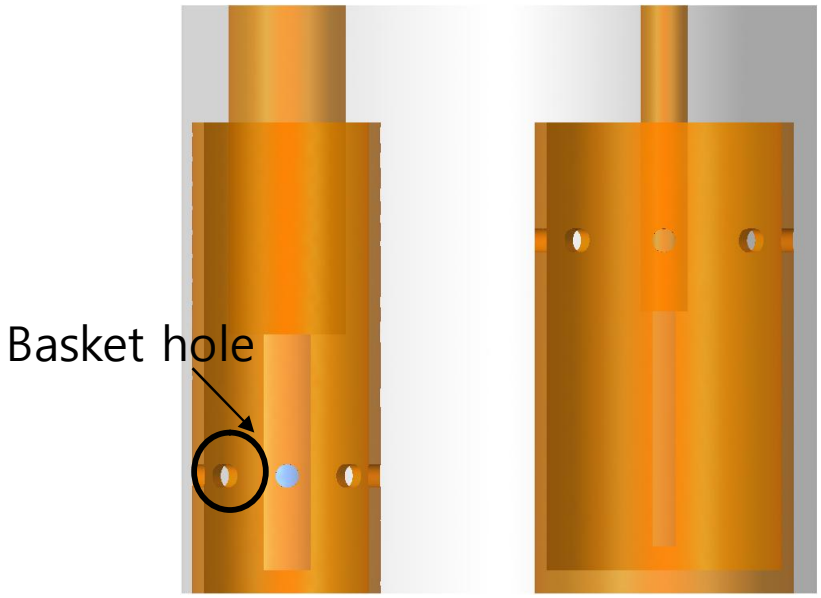

Figure 6.5 basekets around electrodes with holes

Results as shown in Table 6.4 based on configuration at Fig. 6.8 let to the conclusion that Nb contamination and IR-drop can be overcame by adding basket around both anode and cathode.

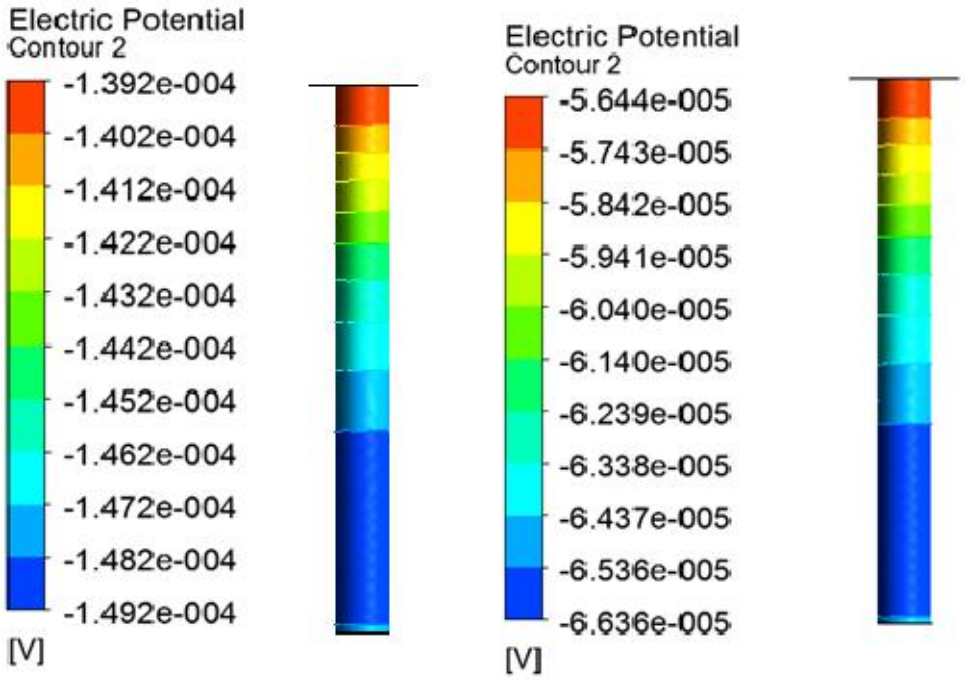

Figure 6.6 Potential distribution on cathode

(left : w/o holes right w/ hole)

Table 6.3 Ohmic drop comparison within this simulation

Index	w/o hole	w/ hole
Lowest Potential(V)	-1.492e-04	-6.636e-05
Highest Potential(V)	-1.392e-04	-5.644e-05

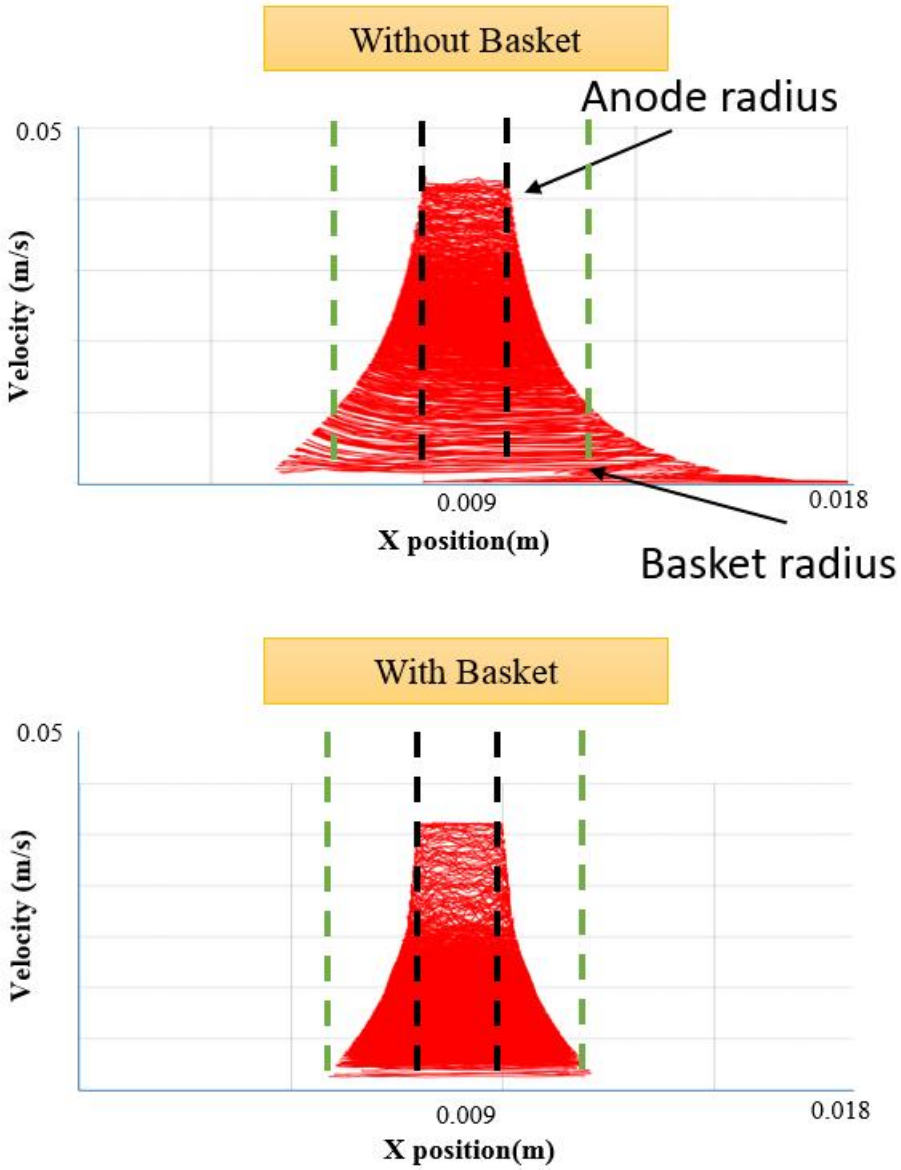

Figure 6.7 Flow velocity comparision around anode (top : w/o basket, bottom : w/ basket)

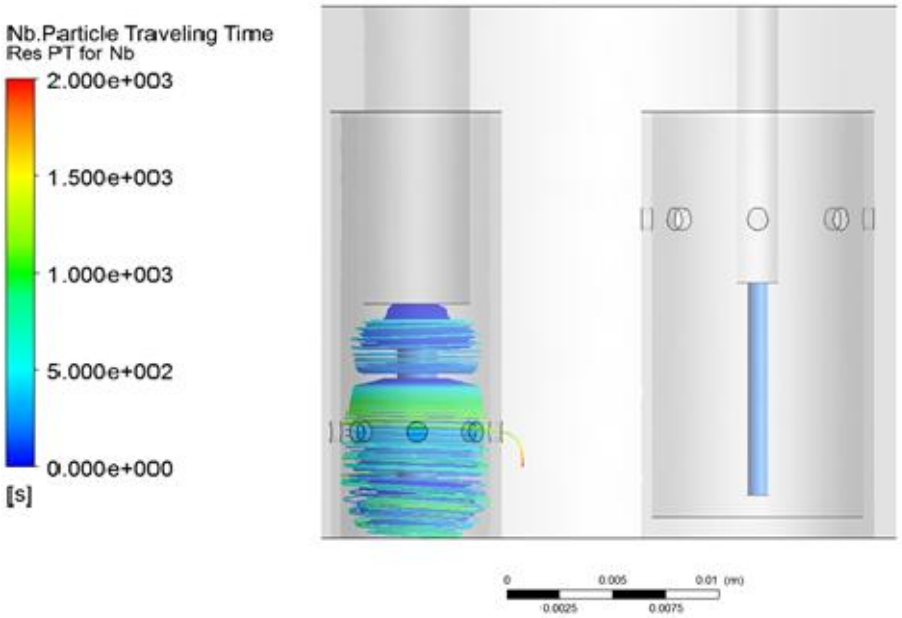

Figure 6.8 particle tracking with basket with holes

Table 6.4 particle tracking result with basket with holes

Particle Elements	**In the Cathode basket**	**In the Anode basket**
Nb	0%	100%
Zr	100%	0%

6.3 Pilot-scale cell design

Table 6.5 is the expected waste mass of decommissioned pressure tube from Wolsong site. If decontamination of pressure tube is too late, additional interim dry storage will be constructed in Wolsong site. Considering the start of decommissioning after 10 years of permanent expiration and minimizing the dry cask, zircaloy should be decontaminated 20 tons annually.

Table 6.5 Wolsong site expiration schedule and mass of pressure tube wastes

Number of Reactors	Lifetime Expiration Date	Pressure Tube waste mass
WOLSONG #1	2018-07	46
WOLSONG #2	2026-11-01	69
WOLSONG #3	2027-12-29	92
WOLSONG #4	2029-02-07	115

However, assuming workday to be 200 days, electrorefining of 20 tons per year through a single hot cell will require 4900A of current. Too high currents are risky for efficiency and risk. Therefore, it is desirable to divide it into 10 hot cells and execute the decontamination process.

Property	Value
Throughput(kg/day)	100
Throughput per second(g/s)	1.16
Molar electrodeposition amount per second (mole/s)	0.0126875
Current (C/s = A)	4896.64

10 cell Units

Property	Value
Throughput(kg/day)	10
Throughput per second(g/s)	0.12
Molar electrodeposition amount per second (mole/s)	0.00127
Current (C/s = A)	490
Voltage (V)	0.4
Watt (W)	100

6.3.1 Economic validation

The economic effects of CANDU decommissioned pressure tube decontamination were analyzed. According to France's radioactive waste disposal strategy, the decommissioned pressure tube contains a long-lived nuclide called Nb-94 and is classified as LL-ILW.

Table 6.6 Radioactive waste disposal strategy of France

	Short-lived Nuclide (Life time under 30yr) wastes	**Long-lived Nuclide (Life-time over 30yr) wastes**
LLW	Surface Disposal	Under 100m Disposal
ILW		
HLW		Deep Geological Disposal

Accordingly, the decontamination effect on the disposal cost of the decontamination process was calculated on the following assumptions.

ILW with Nb repository : Cigéo(France)

1. 1 drum($0.2m^3$) disposal cost : ***₩ 4.3x10^8***
2. Waste density : $7620kg/m^3$

LLW repository : Gyeong-ju 1st Repository

1. drum($0.2m^3$) disposal cost : ***₩ 1.4x10^7***
2. Waste density : $7620kg/m^3$

Therefore, when the decommissioned pressure tube is decontaminated, the amount of ILW will be reduced from 184 tons to 5 tons, which is

expected to have an economic effect of KRW 28 billion. It is also expected that there will be an enormous amount of additional economic benefit if additional costs are to be reduced, such as interim storage construction costs for interim storage of pressure tubes, and additional decontamination process of other ILW metal waste into LLW using the same facility.

Table 6.7 comparison for disposal cost each scenario

	w/ Decontamination	**w/o Decontamination**
ILW(ton)	5	184
LLW(ton)	179	0
COST(₩)	**2 Billions**	**30 Billions**

7. Conclusions and Future work

7.1. Conclusion

The main goal of this study is to develop a decontamination process of making decommissioned CANDU pressure tube into LLW from ILW. Because of high Nb composition in Zr-2.5Nb, long-lived nuclide Nb-94 is contained in decommissioned pressure tube. It makes decommissioned CANDU pressure tube. cannot be disposed of Gyeong-ju LILW repository. To dispose CANDU pressure tube in Gyeong-ju repository, decontamination factor 75,100 should be obtained with new process. This goal was obtained by ORIGEN-2. Electrorefining process using chloride molten salt was selected as a best method for CANDU pressure tube decontamination in view of efficiency and safety.

For electrorefining, redox mechanism has been checked for design process. By cyclic voltammetry experiments, electrochemical parameters of Zr and Nb was determined. During cyclic voltammetry, apparent reduction potential and diffusion coefficient was obtained. Because of positive oxidation of Nb related to Zr, electrorefinig for Zr-Nb separation seems reasonable.

By 1-D electrorefining simulation using REFIN code, element behavior during electrorefining process was confirmed. By using this result, to get high decontamination factor(DF) by electrorefining experiment, potentiostatic methods was used suppressing Nb metal oxidation

reaction. It was confirmed by lab-scale experiments that high decontamination factor(10000~200000) can be obtained by conducting electrorefining on Zr-2.5Nb. It means that decommissioned pressure tube can be converted into LLW by pyrochemical electrorefining process,

However, if we makes pilot or commercialized experiments or process, rotating electrodes should be considered because of Nb droplets intrusion into deposited Zr basket. By ANSYS-CFX tool, it is shown that two main issue(Nb droplets, ohmic drop) can be solved by installing baskets with holes for both anode and cathode

The economic validation of entering the pilot or commercialized process to be designed are considered. The economic reduction for disposal cost was 28 billions KRW. It may increased with considering additional cost of interim storage when CANDU pressure tube is not decontaminated.

The development of the commercialization process is not complete and there are many problems to be solved. But, with this thesis, it is concluded that this new developed process can be a solution to radioactive wastes, a very big problem in the nuclear industry.

7.2. Future Work

This dissertation shows that Zr-Nb can be fully separated from each other. But, for pilot or commercialized process, additional studies should be conducted as follows.

1. A deep study of the behavior of niobium in molten salt.
   - Lack of electrochemical parameters for sophisticated process.
2. Study of material properties of the material to be left in the anode after process
   - Studies to prevent contamination of the Nb complexes in fluid with flow

3. Cell design for pilot-scale electrorefining process and additional experiments.
   - Nb droplets or ohmic drop problem in pilot scale should be checked.

4. Process to separate the deposited materials from the molten salt.
   - Processes for converting ZrCl into Zr metal and separation Zr from molten salt is necessary.

If these issues are solved, pyrochemical decontamination process can be commercialized.

APPENDIX I. ORIGEN-2 INPUT

(CANDU Pressure Tube simulation)

```
-1
-1
-1
RDA *    CANDU Pressure Tube Irradiation
RDA **    CROSS SECTION LIBRARY = CANDUNAU.LIB
CUT         5 1.0E-10 7 1.0E-10 9 1.0E-10 -1
LIP         0 0 0
RDA                          DECAY    LIB              XSECT    LIB
VAR. XSECT
LIB         0        1  2  3          401  402  403        9      50      0      1
21
RDA          PHOTON LIB
PHO         101 102 103    10
TIT    INITIAL COMP. OF UNIT AMOUNTS OF FUEL AND
STRUCTURAL MAT'LS
RDA         READ Zr-2.5Nb including impurities (1000kg)
INP         -1    1    -1    -1    1    1
TIT         IRRADIATION OF ONE METRIC TON OF PWR FUEL
MOV         -1 1 0 1.0
PCH         1    1    1
HED         1    CHARGE
BUP
IRF 10950      1.00E+14    1        2    4 2
BUP

OPTL           8 8 8 8 7 8 7 8 7 8 8 8 8 8 8 8 8 8 8 8 8 8
```

```
   OPTA          8 8 8 8 7 8 7 8 7 8 8 8 8 8 8 8 8 8 8 8 8
   OPTF          8 8 8 8 7 8 7 8 7 8 8 8 8 8 8 8 8 8 8 8 8
   OUT       2       1         -1        0

   MOV       2       1       0      1.0

   DEC               1.0     1     2     5     2
   DEC               3.0     2     3     5     0
   DEC               5.0     3     4     5     0
   DEC               7.0     4     5     5     0
   DEC              10.0     5     6     5     0
   DEC              30.0     6     7     5     0
   DEC              50.0     7     8     5     0
   DEC              70.0     8     9     5     0
   DEC             100.0     9    10     5     0
   OPTL          8 8 8 8 7 8 7 8 7 8 8 8 8 8 8 8 8 8 8 8 8
   OPTA          8 8 8 8 7 8 7 8 7 8 8 8 8 8 8 8 8 8 8 8 8
   OPTF          8 8 8 8 7 8 7 8 7 8 8 8 8 8 8 8 8 8 8 8 8
   OUT            10       1         -1        0
   END
4  400000  9.7240E+05  410000  2.5000E+04  130000  7.5000E+01
050000 5.0000E-01
4 480000 5.0000E-01 060000 2.7000E+02 240000 1.0000E+02 270000
2.0000E+01
4  290000  5.0000E+01  720000  5.0000E+01  010000  1.0000E+01
260000 1.5000E+03
4  120000  2.0000E+01  250000  5.0000E+01  420000  5.0000E+01
280000 7.0000E+01
```

4 070000 6.5000E+01 150000 2.0000E+01 140000 1.0000E+02 500000 5.0000E+01

4 740000 5.0000E+01 220000 5.0000E+01 920000 3.5000E+00 0 0 0

APPENDIX II. REFIN INPUT

(Charpt 5.1 condition)

Radioactive Zr-2.5Nb CANDU PT after 10 years cooling

```
&input1 nelemt=9, a_type=0, temp=773.d0,
   ename = 'Zr', 'Nb', 'ef', 'Cr', 'Co',
'Ni', 'Li', 'Ka' 'Cl',
   stde = 2.186d0, 1.472d0, 1.388d0, 1.641d0, 1.207d0,
1.011d0, 3.900d0, 4.200d0, 0.000d0,
   diffu1= 1.000d-6, 1.00d-6, 1.00d-6, 1.00d-6, 1.00d-6,
1.000d-6, 1.00d-6, 1.00d-6, 1.0d-6,
   diffu2= 1.133d-5, 2.6d-6, 1.38d-5, 1.63d-5, 3.74d-5,
1.500d-5, 2.5d-5, 2.5d-5, 2.5d-5,
   curr0 = 1.d-06, 1.d-06, 1.d-06, 1.d-06, 1.d-06,
1.d-06, 1.d-06, 1.d-06, 0.D-10,
   zi = 4.0d0, 3.0d0, 2.0d0, 2.0d0, 2.0d0,
2.0d0, 1.0d0, 1.0d0, -1.d0,
   tca = 0.5d0, 0.5d0, 0.5d0, 0.5d0, 0.5d0,
0.5d0, 0.5d0, 0.5d0, 0.5d0,
   tcc = 0.5d0, 0.5d0, 0.5d0, 0.5d0, 0.5d0,
0.5d0, 0.5d0, 0.5d0, 0.5d0,
   catp=-1.8d0,
   anop=-1.0d0,
   ipset= 1,
   tset= 10000.0d0
   cmaxt= 490d0
   aberr=1.d-40,
```

```
   rlerr=1.d-15,
&
&input2
   del1=1.0d-3,
   del2=1.0d-2,
   del3=1.0d-2,
   del4=1.0d-3,
      dy=1.0d-3,
   area=2400d0, 707d0,
   vol =1552.8d0, 91538.2d0, 0.1d0,
&
&INPUT3
   ISTATE=1,
   ITASK=5,
   epslon=5.d-1,
   iopt=1,
   mxstep=1000,
   h0=1.d-5,
   jt=5,
   ml=26,
   mu=26,
   hmax=600.0d0,
   itol=1,
   rtoli=1.0d-9,
   atoli=1.d-15,
   iprint=2,
&
&input4
```

Can= 9.7368d-01, 2.4624d-02, 1.5086d-03,9.9541d-05, 7.4700d-06, 8.3971d-05, 3.55d-13, 3.67d-14, 1.65d-15,

Cms= 1.870d-03, 4.6624d-34, 4.6624d-34, 4.6624d-34, 4.6624d-34, 4.6624d-34, 7.02d-02, 2.75d-01, 6.36d-01,

Cca= 0.000d-20, 0.000d-20, 0.000d-20, 0.000d-20, 0.000d-20, 0.000d-20, 0.000d-20, 0.000d-20, 0.000d-20, 0.000d-20,

&

&input5

mass=10000d0, 148291.93d0, 0.001d0,

gatom=91.224d0, 92.90638d0, 55.845d0, 51.9961d0, 58.933d0, 58.693d0, 6.941d0, 39.098d0, 35.453d0,

&

Bibliography

Ahluwalia, R., Hua, T.Q., Geyer, H.K., 1999. Behavior of uranium and zirconium in direct transport tests with irradiated EBR-II fuel. Nuclear technology 126, 289-302.

Baboian, R., Hill, D., Bailey, R., 1965. Electrochemical Studies on Zirconium and Hafnium in Molten LiCl-KCl Eutectic. Journal of The Electrochemical Society 112, 1221-1224.

Bard, A., Faulkner, L., 2001. Electrochemical methods: principles and applications. Electrochemical Methods: Principles and Applications.

Cho, I.-J., 2013. Current Status of Pyroprocessing Development at KAERI. SCience and Technology of Nuclear Installations 2013.

Collins, E.D., DelCul, G.D., Spencer, B.B., Brunson, R.R., Johnson, J.A.,Terekhov, D., Emmanuel, N., 2012. Process Development Studies for Zirconium Recovery/Recycle from used Nuclear Fuel Cladding. Procedia Chemistry 7, 72-76.

Fabrian, C.P., Luca, V., Le, T., Bond, A.M., Chamelot, P., Massot, L., Caravaca, C., Hanley, T.L., Lumpkin, G.R., 2013. Cyclic Voltammetric Experiment-Simulation Comparisons of the Complex Mechanism Associated with Electrochemical Reduction of Zr4+ in LiCl-KCl Eutectic Molten Salt. Journal of The Electrochemical Society 160,

H81-H86.

Fujita, R., Nakamura, H., Haruguchi, Y., Takahashi, R., Sato, M., Shibano, T., Ito, Y., Goto, T., Terai, T., Ogawa, S., 2005a. Development of zirconium recovery process for zircaloy claddings and channel boxes from boiling water reactors by electroreˆning in molten salts, ICAPP '05, Seoul, Korea.

Ghosh, S., Vandarkuzhali, S., Venkatesh, P., Seenivasan, G., Subramanian, T., Prabhakara Reddy, B., Nagarajan, K., 2009. Electrochemical studies on the redox behaviour of zirconium in molten LiCl–KCl eutectic. Journal of Electroanalytical Chemistry 627, 15-27.

Groult, H., El Ghallali, H., Barhoun, A., Briot, E., Perrigaud, L., Hernandorena, S., Lantelme, F., 2010. Preparation of Co–Sn alloys by electroreduction of Co (II) and Sn (II) in molten LiCl–KCl. Electrochimica Acta 55, 1926-1932.

Hoover, R.O., Phongikaroon, S., Simpson, M.F., Yoo, T.-S., Li, S.X., 2011. Computational Model of the Mark-IV Electrorefiner: Two-Dimensional Potential and Current Distributions. Nuclear Technology 173, 176-182.

Ibrahim, E., Cheadle, B., 1985. Development of zirconium alloys for pressure tubes in CANDU reactors. Canadian Metallurgical Quarterly 24, 273-281.

Iizuka, M., Inoue, T., Shirai, O., Iwai, T., Arai, Y., 2001. Application of

normal pulse voltammetry to on-line monitoring of actinide concentrations in molten salt electrolyte. Journal of nuclear materials 297, 43-51.

Lee, C.H., Kang, K.H., Jeon, M.K., Heo, C.M., Lee, Y.L., 2012. Electrorefining of Zirconium from Zircaloy-4 Cladding Hulls in LiCl-KCl Molten Salts. Journal of The Electrochemical Society 159, D463-D468.

Park, J., Choi, S., Sohn, S., Kim, K.-R., Hwang, I.S., 2014. Cyclic Voltammetry on Zirconium Redox Reactions in LiCl-KCl-ZrCl4 at 500° C for Electrorefining Contaminated Zircaloy-4 Cladding. Journal of The Electrochemical Society 161, H97-H104.

Park, K.T., Lee, T.H., Jo, N.C., Nersisyan, H.H., Chun, B.S., Lee, H.H., Lee, J.H., 2013. Purification of nuclear grade Zr scrap as the high purity dense Zr deposits from Zirlo scrap by electrorefining in LiF–KF–ZrF4 molten fluorides. Journal of Nuclear Materials 436, 130-138.

Sakamura, Y., 2004. Zirconium behavior in molten LiCl-KCl eutectic. Journal of The Electrochemical Society 151, C187-C193.

Yamada, D., Murai, T., Moritani, K., Sasaki, T., Takagi, I., Moriyama, H., Kinoshita, K., Yamana, H., 2007a. Diffusion behavior of actinide and lanthanide elements in molten salt for reductive extraction. Journal of Alloys and Compounds 444, 557-560.

Yamada, D., Murai, T., Moritani, K., Sasaki, T., Takagi, I., Moriyama,

H., Kinoshita, K., Yamana, H., 2007b. Diffusion behavior of actinide and lanthanide elements in molten salt for reductive extraction. Journal of Alloys and Compounds 444–445, 557-560.

초 록

지르코늄은 낮은 열중성자 흡수단면적과 내부식에 대한 강한 저항성을 가지고 있는 우수한 물질이다. 여기에 지르코늄에 나이오븀을 녹여만든 지르코늄 합금은 지르코늄 금속의 취약점인 수소취화 문제에 대한 강한 저항성을 더해줌으로써 매우 고온, 고압, 고방사선의 중수로의 압력관 등 다양한 영역에 활용되고 있다. 그러나, 나이오븀의 이러한 장점에도 불구하고, 높은 방사선 하에 Nb-94를 대량으로 만들어내는 문제점이 발생되었고, Nb-94는 긴 반감기와 강한 방사성으로 인해 압력관 폐기물의 처리가 매우 어려워지게 되었다. 과거 압력관 교체로 이미 23톤의 압력관이 중간저장이 이루어지고 있으며, 앞으로 이루어질 월성 원자력발전소의 정지에 따라 향후 2029년까지 최소 115톤에서 많게는 180톤까지의 압력관 해체 폐기물이 나올 예정이다. 현재 국내의 처분장으로는 중수로 압력관 폐기물을 처분할 수 없기 때문에, 이에 대한 제염 또는 처분 연구가 이루어져야 한다. 이에따라 중수로 압력관의 처분을 위한 제염공정 통해 저준위폐기물로 만들 수 있다면 압력관 뿐 아니라 다양한 곳에서 이용되고 있는 지르코늄 합금 해체폐기물에 대한 해결책을 제시할 것으로 기대된다.

이러한 이유로 압력관을 제염하기 위한 공정연구가 이루어져 왔는데, 2009년 발표된 표면제염 연구는 제염물질의

침투두께의 한계에 의해서 지르코늄 합금 내부에 균일하게 분포해 있는 나이오븀을 분리해내기는 어려울 것으로 여겨지며, 아이오다인을 이용한 체적제염 또한 공정효율성이 떨어져 선호되지 않는다. 가장 적절한 공정은 전해정련 공정으로 여겨지고 있으며, 불화물이나 염화물과 같은 전해공정이 가장 깊은 연구가 진행되고 있다. 불화물의 경우 전해공정시 큰 입자형태의 전착물을 회수 할 수 있는 장점이 있으나, 높은 공정온도와 부식문제로 인해 대규모공정시 안전성이 우려된다. 이에 따라 염화물을 사용하는 공정은 불화물에 비해 낮은 온도에서 부식문제도 적은 상태의 공정을 수행할 수 있기 때문에 상용 공정에 적합하다. 그러나 염화염의 경우 지르코늄및 나이오븀의 전착물 거동이 복잡한 단점이 있기에 이에 대한 공정연구가 진행되어야 한다.

본 논문에서는 염화염에서 지르코늄과 나이오븀의 산화환원 거동을 바탕으로 전해정련을 통한 지르코늄과 나이오븀을 분리하여 지르코늄 합금을 제염시키는 연구를 진행하였다. 이를 위해 ORIGEN-2를 이용하여 압력관의 방사화 계산을 수행, Nb-94의 방사선 농도를 알아냈고 이에 따른 제염계수 목표를 75,100으로 설정하였다.

전해정련공정을 위해서는 염화염 내에서의 지르코늄 나이오븀의 산화환원 거동을 파악하여야 한다. 이를 위해 순환전류법을 통해 산화환원 거동과 열역학적 데이터를 수집하였고, 문헌과 비교하였을때 일치하는 것을 확인하였다. 지르코늄금속의 산화전위가 나이오븀의 산화전위보다 낮지만, 나이오븀 이온의 나이오븀 금속으로의 환원전위가 지르코늄의

경우보다 매우 높기 때문에, 나이오븀의 산화를 억제시켜야 한다. 이에 근거하여 먼저 1-D 전해정련 계산코드인 REFIN을 이용하여 각 원소들의 거동을 파악하였고, LiCl-KCl-$ZrCl_4$염을 이용한 전해정련 공정을 설계하였다.

과거의 실험에서는 전해정련시 지르코늄 합금에 균일하게 녹아있는 나이오븀의 석출에 대해서는 고려를 하지 않았기 때문에 이번 실험에서는 이를 분리해내기 위해 basket을 추가 설치하여 물리적으로 나이오븀 particle들과 지르코늄 전착물을 분리하였다. 전착물은 배스킷 내부에 전착되었고, 염에 전착물들이 불균형하게 존재하였던 것과 달리 배스킷 내부에 고르게 전착되었던 것을 확인하였다. 또한, ICP-MS를 활용한 조성 분석결과를 통해 높은 순수도의 지르코늄을 회수하였으며 Nb에 대해 충분히 높은 10000~200000의 높은 제염계수를 획득함으로써 전해정련을 통한 CANDU 압력관 해체폐기물의 저준위화공정을 수행할 수 있음을 실험실 규모에서 실험에서 확인하였다.

그러나 실제 실험에서는 한계전류와 확산층의 제어를 위해 회전전극을 사용하게 된다. 이러한 경우에는 전해질 내에 유동이 발생하여 Nb 입자들이 지르코늄 전착물에 오염이 될 수 있다. 이를 방지하기 위해서는 추가적인 basket설치가 필수적으로 이루어져야 할 것이다. 그러나 basket을 설치하게 된다면 추가적인 전압강하등의 요소로 인해 전력효율이 떨어지게 된다. 이를 해결하기 위해 basket에 구멍을 뚫은 cell을 가정하여 CFX-ANSYS를 이용하여 유체내 입자거동해석 및 전압강하에 대한 시뮬레이션을 수행하였고, 이러한 basket을

통하여 효율적인 전해셀을 설계할 수 있음을 파악하였다.

이러한 연구결과를 통해 Pilot-scale 및 상업규모의 설계가 만들어지게 된다면, 처분비용만 280억 이상의 감소와 중간저장시설 등의 추가비용이 감소할 것으로 여겨진다.

주요어 : 압력관, 지르코늄, 나이오븀, 전해정련
학 번 : 2017-24335